

A Novel Risk-based Design Criteria for Urban Heat Island:

A Case Study of Kempten, Germany

in partial fulfillment of the requirements for the degree of
Master of Science at the TUM School of Engineering and Design of the
Technical University of Munich.

Supervised by Roland Reitberger, M.Eng. and Farzan Banihashemi, M.Sc.
Institute of Energy Efficient and Sustainable Design and Building

Submitted by Joshua Huang
Arcisstr. 21
80333, München

Submitted on Munich, 17.06.2022

Agreement (Vereinbarung)

zwischen

der Technischen Universität München, vertreten durch ihren Präsidenten,
Arcisstraße 21, 80290 München

hier handelnd der Lehrstuhl für Energieeffizientes und Nachhaltiges Planen und Bauen
(Univ.-Prof. Dr.-Ing. W. Lang), Arcisstr. 21, 80333 München

– nachfolgend TUM –

und

Frau/Herrn

(Anschrift)

– nachfolgend Autorin/Autor –

Die Autorin / der Autor wünscht, dass die von ihr/ihm an der TUM erstellte Masterarbeit mit dem Titel

.....

.....
 auf mediaTUM und der Webseite des Lehrstuhls für Energieeffizientes und Nachhaltiges Planen und Bauen mit dem Namen der Verfasserin / des Verfassers, dem Titel der Arbeit, den Betreuer:innen und dem Erscheinungsjahr genannt werden darf.

in Bibliotheken der TUM, einschließlich mediaTUM und die Präsenzbibliothek des Lehrstuhls für Energieeffizientes und Nachhaltiges Planen und Bauen, Studierenden und Besucher:innen zugänglich gemacht und veröffentlicht werden darf. Dies schließt auch Inhalte von Abschlusspräsentationen ein.

mit einem Sperrvermerk versehen und nicht an Dritte weitergegeben wird.

(Zutreffendes bitte ankreuzen)

Zu diesem Zweck überträgt die Autorin / der Autor der TUM zeitlich und örtlich unbefristet das nichtausschließliche Nutzungs- und Veröffentlichungsrecht an der Masterarbeit.

Die Autorin / der Autor versichert, dass sie/er alleinige(r) Inhaber(in) aller Rechte an der Masterarbeit ist und der weltweiten Veröffentlichung keine Rechte Dritter entgegenstehen, bspw. an Abbildungen, beschränkende Absprachen mit Verlagen, Arbeitgebern oder Unterstützern der Masterarbeit. Die Autorin / der Autor stellt die TUM und deren Beschäftigte insofern von Ansprüchen und Forderungen Dritter sowie den damit verbundenen Kosten frei.

Eine elektronische Fassung der Masterarbeit als pdf-Datei hat die Autorin / der Autor dieser Vereinbarung beigefügt. Die TUM ist berechtigt, ggf. notwendig werdende Konvertierungen der Datei in andere Formate vorzunehmen.

Vergütungen werden nicht gewährt.
Eine Verpflichtung der TUM zur Veröffentlichung für eine bestimmte Dauer besteht nicht.

Die Autorin / der Autor hat jederzeit das Recht, die mit dieser Vereinbarung eingeräumten Rechte schriftlich zu widerrufen. Die TUM wird die Veröffentlichung nach dem Widerruf in einer angemessenen Frist und auf etwaige Kosten der Autorin / des Autors rückgängig machen, soweit rechtlich und tatsächlich möglich und zumutbar.

Die TUM haftet nur für vorsätzlich oder grob fahrlässig verursachte Schäden. Im Falle grober Fahrlässigkeit ist die Haftung auf den vorhersehbaren Schaden begrenzt; für mittelbare Schäden, Folgeschäden sowie unbefugte nachträgliche Veränderungen der veröffentlichten Masterarbeit ist die Haftung bei grober Fahrlässigkeit ausgeschlossen.

Die vorstehenden Haftungsbeschränkungen gelten nicht für Verletzungen des Lebens, des Körpers oder der Gesundheit.

Meinungsverschiedenheiten im Zusammenhang mit dieser Vereinbarung bemühen sich die TUM und die Autorin / der Autor einvernehmlich zu klären. Auf diese Vereinbarung findet deutsches Recht unter Ausschluss kollisionsrechtlicher Regelungen Anwendung. Ausschließlicher Gerichtsstand ist München.

München, den _____, den _____

.....
.....
(TUM) (Autor:in)

Declaration (Erklärung)

Ich versichere hiermit, dass ich die von mir eingereichte Abschlussarbeit selbstständig verfasst und keine anderen als die angegebenen Quellen und Hilfsmittel benutzt habe.

Ort, Datum, Unterschrift

Acknowledgements

This paper would not have been possible without the continuous support and advice from my supervisors, Roland Reitberger, M.Eng. and Farzan Banihashemi, M.Sc. I would also like to thank my supervisors and my colleague Egi Kalaj for helping me with the details and sharing resources related to the case study area. Specifically, Egi Kalaj helped me to understand details of the UWG and provided me with the UHI modelling parameters. She has also independently confirmed some of the UHI values in this paper with her own research.

Regarding the risk analysis aspects of this paper, I would like to first thank Dr. Eun Jeong Cha and Dr. Paolo Gardoni from the University of Illinois Champaign-Urbana for inspiring me in the field of engineering risk analysis. From the TUM Engineering Risk Analysis Group I would like to thank Dr. Daniel Straub for all his lectures and notes that formed the basis of the risk aspects of this paper and Max Teichgräber, M.Sc, who advised me on some of the risk analysis aspects of this paper.

I would like to thank Dr. Stefan Muthers and Axel Kuschnerow from DWD for helping me with the meteorological aspects of this paper. Dr. Susanne Breitner from the LMU IBE-Chair of Epidemiology was instrumental in helping me to establish a useable temperature-mortality relationship, which was a major part of this paper. I'd also like to thank Dr. Andreas Krause from the TUM Professorship for Land Surface-Atmosphere Interactions for guiding me on climate change topics that were in the preliminary version of this paper but will be saved for future work.

Table of Contents

Agreement (Vereinbarung).....	I
Declaration (Erklärung)	III
Acknowledgements	IV
Table of Contents	1
Abstract	4
List of Variables.....	5
List of Abbreviations	6
Glossary	7
1. Introduction	8
1.1. Background	8
1.2. Need for a Risk-based Design Criteria	9
1.3. Research Aim	9
1.3.1. Scope	10
1.3.2. Structure	10
2. State of the Art	11
2.1. Extreme Heat and UHI	11
2.2. UHI Design Criteria.....	13
2.3. Design Codes and Risk Criteria	13
3. Method	18
3.1. Study Area.....	18
3.2. Meteorological Data.....	20
3.3. Mortality Data	20
3.4. Resistance.....	21
3.4.1. FN Curves	21
3.4.2. Statistical Analysis.....	22
3.4.3. Exposure-Response	24
3.5. Load.....	27
3.5.1. UHI Modelling.....	27
3.5.2. Statistical Analysis.....	29
4. Results	30
5. Discussion.....	35
5.1. Resistance.....	35
5.2. Load.....	35

5.3. Practical Application.....	37
6. Conclusion.....	38
References.....	41
List of Figures.....	49
List of Tables.....	50
Appendix.....	51
A.1. Weather Data.....	51
B.1. Sample MATLAB Script.....	53
B.2. Sample Grasshopper (Ladybug Tools) Script.....	56
B.3. Building Model of Study Area.....	59
C.1. Climate Models for Future Scenarios.....	60

*“The cities of tomorrow are
being planned today.”*

Abstract

Introduction: Studies on urban heat island (UHI) have increased over the past decades and have mainly focused on topics such as thermal comfort, building energy, and sensitivity studies. Also, research on extreme heat or heatwaves has become an increasingly popular research topic since the turn of the century and is related to UHI. However, there is currently a research gap in the development of risk-based design criteria for UHI.

Objectives: This paper proposed a risk-based UHI design criteria by accounting for heat-related mortality risk.

Methods: The design criteria was developed based on the annual hottest seven-day mean temperatures. FN curves were used to quantify tolerable levels of societal risk which have also been used by other regulatory authorities. Published exposure-response relationships for temperature and mortality for southern Germany were also used to determine the regional heat mortality rate. These two processes were combined to obtain a maximum allowable UHI intensity (UHII), $UHII_{design}$ for several risk scenarios. This design value was compared to the 50-year UHII, $UHII_{tot,50}$ for a residential district in Kempten, Germany by using the Urban Weather Generator. If $UHII_{tot,50}$ did not exceed $UHII_{design}$, then the analyzed area was considered adequate.

Results: The $UHII_{tot,50}$ of the study area was 0.17°C . This met $UHII_{design}$ in all the risk scenarios. This was to be expected since the study area had a relatively low urban density.

Conclusions: A risk-based UHI design criteria for UHI that quantifies mortality risk has been developed and demonstrated for the city of Kempten. This research lays the foundation for decision-makers and urban planners to incorporate precise UHI design targets without over- or under-design.

Keywords: urban heat island; design criteria; heat mortality; temperature

List of Variables

$\lambda_{D,Tolerable}$	Tolerable annual individual fatality rate
b	Constant representing level of risk aversion
F	Frequency of an event
N	Number of fatalities
$N_{tolerable}$	Tolerable number of fatalities
$N_{R,max}$	Limiting number of fatalities
P	Population
tas	hottest week air temperature at two meters
tas_{50}	50-year hottest week air temperature at two meters
UHI_{50}	50-year hottest week UHI temperature
$UHI_{existing,50}$	50-year hottest week UHI temperature due to existing conditions
$UHI_{new,50}$	50-year hottest week UHI temperature due to new development
$UHI_{tot,50}$	$UHI_{existing,50} + UHI_{new,50}$
$UHII_{50}$	50-year hottest week UHII
$UHII_{design}$	Maximum allowable 50-year hottest week UHII
$UHII_{existing,50}$	50-year hottest week UHII due to existing conditions
$UHII_{new,50}$	50-year hottest week UHII due to new development
$UHII_{total,50}$	$UHII_{existing,50} + UHII_{new,50}$

List of Abbreviations

ALARP	As low as reasonably practicable
ASCE	American Society of Civil Engineers
DWD	Deutscher Wetterdienst
ECCS	European Convention for Constructional Steel Work
IPCC	Intergovernmental Panel on Climate Change
NOAA	National Oceanic and Atmospheric Administration's
UHI	Urban heat island
UHII	Urban heat island intensity
UWG	Urban Weather Generator

Glossary

ALARP: The reduction of risk to a reasonably practicable level at which the costs of further reduction of risk would be highly disproportionate to the benefits gained

Façade-to-site ratio: The ratio of the sum of all the vertical surfaces of structures to the plan area of the site being analyzed

Footprint density: The ratio of the sum of all plan areas of structures to the plan area of the site being analyzed

Hottest week: The highest seven-day rolling air temperature mean in a year

Load: The urban heat island intensity caused by an urban area

Percentage of green: Percentage of a given plan area that is covered by vegetation

Resistance: The maximum allowable urban heat island intensity

Return period: The statistically determined average time between two events

Sensible anthropogenic heat: Waste heat discharged into a given area caused by anthropogenic activities that are not a result of phase changes

Tree coverage: Percentage of a given plan area that is covered by trees

Urban Heat Island: An urban area which is warmer than surrounding rural areas due to anthropogenic factors

Urban Heat Island Intensity: The difference between temperatures in the urban area and the surrounding rural areas

1. Introduction

1.1. Background

As the 21st century progresses, trends in urbanization and climate change and their compounded effects are increasingly affecting society. The urban heat island (UHI) effect is a phenomenon that is influenced by these trends. UHI is defined as the higher temperatures that occur in an urban area compared with the surrounding rural areas due to anthropogenic factors (IPCC, 2021). There is typically a diurnal pattern in which the highest temperature difference occurs at night and the lowest differences during the day. The UHI intensity (UHII) or the difference between temperatures in the surrounding rural areas and the urban area is known to be approximately 2 to 4 °C in most cases, although in extreme cases temperature differences can be up to 5 to 10 °C (Heaviside, Macintyre & Vardoulakis, 2017; Hibbard et al., 2017).

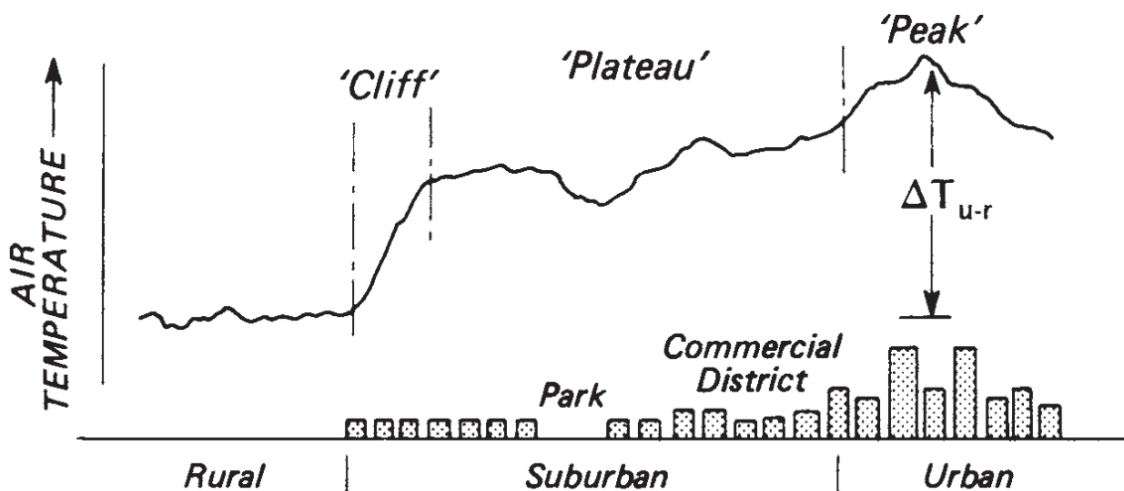


Figure 1-1: Typical distribution of temperatures in UHI (Figure 8.12 from Oke, 1987)

UHI is being impacted by rising urbanization and the increase of extreme temperatures due to climate change. Regarding urbanization, 68% of the global population is expected to live in urban areas by 2050 (DESA, 2019). Furthermore, it is projected that 75% of the infrastructure needed by 2050 is yet to be built (Egler and Frazao, 2016), and most of the demand for infrastructure will be in urban areas (CCFLA, 2015). How these trends affect UHI are linked closely to the density of urban morphology (Ibrahim et al., 2021; Nakano et al., 2015; and Salvati, Massimo and Inostroza, 2017).

Furthermore, UHI is also related to the air temperature, and a trend of particular concern is the increase of extreme heat and heat waves due to climate change. Europe has already experienced a number of record-breaking heat waves in the 21st century that have caused tens of thousands of deaths, such as in 2003 in central Europe and in 2010 in Russia (Barriopedro et al., 2011; Russo et al., 2015). The frequency and intensity of heat waves are only expected to increase with climate change (IPCC, 2021). In Europe and the U.S., extreme heat is the leading cause of climate-related deaths in the past 30 years (NOAA, 2020; EEA, 2022). The effects of extreme temperatures and heat waves due to climate change are further worsened by UHI.

1.2. Need for a Risk-based Design Criteria

In light of increased urbanization and climate change, the risk of heat-related mortality is expected to rise in the coming years unless proper action is taken. Studies estimate that the heat-related mortality rates in Europe could increase by over 50% by 2050 (Ortu et al. 2019; Rohat et al., 2019). How designers plan for UHI will have considerable influence over how tomorrow's cities cope with heat-related mortality. This is reflected by the transition of UHI research trends in the past decade from anthropogenic and meteorological causes to building- and health-related topics (Wu and Ren 2018).

It is common practice for civil engineering design standards to set risk-based minimum design loads of environmental effects on infrastructure such as snow and wind (ASCE, 2017; CEN, 2003 and 2005). However, design targets based on acceptable risk are lacking for UHI. Current practice such as mandates on eco-roofs (Planning and Zoning, Code of the City of Portland, 2020), tree shading requirements (Tree Shading Requirements for Parking Lots, Sacramento City Code, 2021), vegetative cover requirements (Green Factor Measurements, City of Seattle Municipal Code, 2021), and recommendations on urban morphology (Planning Dept. HK, 1993) do not define a risk-based design target. As a result, the engineering community has called for the development of clear risk-based UHI design targets in recent years (Coseo and Larsen, 2015; Heaviside, Macintyre and Vardoulakis, 2017; Sailor et al., 2016).

1.3. Research Aim

This paper answered the following research question: How can design criteria be developed for UHI using acceptable risk targets? The authors believed that by using

similar methods to develop design criteria that have been used in practice for other civil engineering applications for the past several decades, a useable design criteria could be formulated. Furthermore, in the context of the case study area outlined in this paper, it was not expected to be close to exceeding any design criteria that were to be developed due to its relatively low urban density.

The goal of this paper was to develop a novel risk-based design criteria by incorporating the excess heat-related mortality risk due to UHI. The developed design criteria provided concrete thresholds to which UHI should be limited. This was demonstrated for a case study area in Kempten, Germany. This paper is an initial contribution to the development of a design criteria for UHI, and more work in the future is needed to implement it into design processes.

1.3.1. Scope

The UHI design criteria was developed using extreme value statistical methods and societal risk concepts that are commonly used in civil engineering design applications such as for environmental loads on buildings, dam failures, landslides and tunnel safety. The design criteria was developed in the context of southern Germany (Baden-Württemberg and Bavaria) and demonstrated for a case study area in Kempten, Germany. This paper used the seven-day mean temperature as the basis for the design criteria since research has shown that it correlates better with the mortality rate of southern Germany. The focus of the design criteria was on excess heat mortality risk, and the resistance and load values were developed based on this.

1.3.2. Structure

[Section 2](#) reviews the scientific basis of extreme heat and UHI and some current design practices for UHI. These current practices were compared with the current state of design codes and standards used for some civil engineering applications such as snow and wind loads. [Section 3](#) outlines the methodology to develop a risk-based design criteria for, detailing the use of extreme value statistics to analyze meteorological data and the use of societal risk concepts. In [section 4](#), the results of developing the design criteria applied to the study area are presented. [Section 5](#) discusses the results of this case study and its significance for urban design. Finally, [section 6](#) provides a summary, presents some limitations of this paper, and provides a direction for future research.

2. State of the Art

2.1. Extreme Heat and UHI

Extreme heat and UHI have been popular research topics within the last decade. The body of literature is vast, ranging from climate change to meteorological aspects to effects on human health. Trends of number of publications and key words in publications on heatwaves since 1990 are shown in Figure 2-1 and Figure 2-2. This section reviews the some of the literature on the scientific basis for extreme heat and UHI that are relevant to this study.

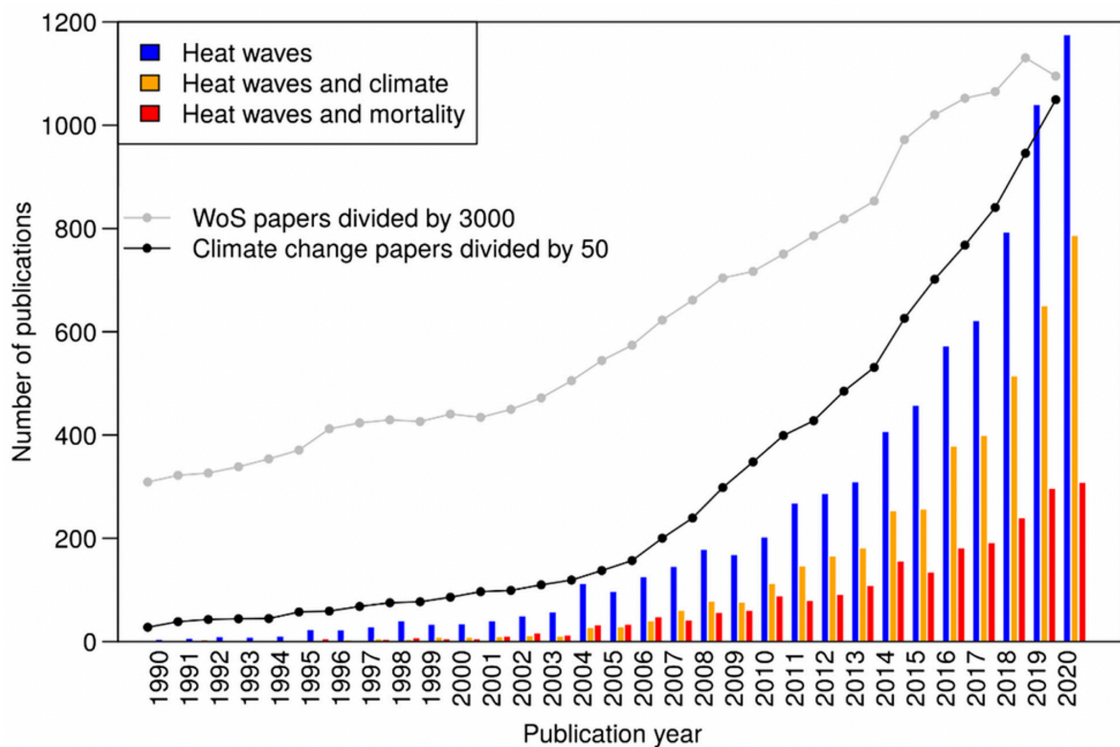


Figure 2-1: Trend of publications on heatwaves (Fig.1 from Marx, Haunschild and Bormmann, 2021)

liferated rapidly. Much of the research has centered on optimization of urban areas to mitigate UHI or understanding factors that cause UHI. There are even studies that investigate optimizing vegetation species, such as by Rahman et al. (2017). There are also numerous sensitivity studies of parameters affecting UHI. Banihashemi, Reitberger and Lang (2022), Ibrahim et al. (2021), Nakano et al. (2015), and Salvati, Massimo and Inostroza (2017) have all studied sensitivities of model parameters for Kempten, Germany, Cairo, Egypt, Boston, U.S., and the Mediterranean region respectively, using the Urban Weather Generator (UWG). Research on UHI using ENVI-met are even more numerous.

2.2. UHI Design Criteria

Although research on understanding UHI behavior is relatively mature, development of concrete, risk-based UHI temperature design targets are lacking. As mentioned before, there are research on temperature and relative mortality risk, but the research does not define what an acceptable level of risk is in a design context. The current state of UHI design consist mainly of guidelines and codes that address UHI mitigation as a goal or as a byproduct of other goals such as mandates on eco-roofs (Planning and Zoning, Code of the City of Portland, 2020), tree shading requirements (Tree Shading Requirements for Parking Lots, Sacramento City Code, 2021), vegetative cover requirements (Green Factor Measurements, City of Seattle Municipal Code, 2021), and recommendations on urban morphology (Planning Dept. HK, 1993). However, all these methods do not use risk-based design criteria.

2.3. Design Codes and Risk Criteria

Currently, there is a lack in adequately addressing UHI design from a risk-based perspective. However, it is helpful to review the statistical basis of how design codes and standards have been developed in other civil engineering applications in order to develop a design criteria for UHI.

In Europe, EN 1991 sets forth standards for loads and actions on structures (CEN, 2003). ASCE 7 is the American equivalent for design loads for structures (ASCE, 2017). These two sets of codes represent the investment of a significant locus of research on effects of environmental load on structures. They both use extreme value statistics to determine the design loads. This is done by determining the probability

distribution of data from meteorological or geophysical observations. From the probability distribution, the design load based on the selected return period is obtained. This process is repeated for different locations and load maps are constructed by grouping climatologically similar regions together (see Figure 2-3). The design load is multiplied by other factors to account for different situations (building occupancy type, building shape, etc.). This methodology has gone through only minor changes in the past few decades.

With snow loads in ASCE 7, the basis for the extreme value statistical analysis was taken from Ellingwood and Redfield (1983). The snow load maps were provided by O'Rourke, Koch, and Redfield (1983) and have only gone through minor updates as more recent meteorological observations became available. One major change that is currently being discussed is the use of a uniform risk approach rather than a uniform hazard approach (Buska, Greatorex, and Tobiasson, 2020). The earthquake section of ASCE 7 already uses the uniform risk approach. The wind load section in ASCE 7 has gone through more changes. The extreme value statistical analysis from Peterka (1992) and Peterka and Shahid (1993 and 1998) were used and updated as more recent meteorological observations became available. In ASCE 7-16, the latest release of ASCE 7, non-hurricane wind loads were further categorized as storm or non-storm with different probability distributions (Lombardo, Main, and Simiu, 2009). The model used to determine hurricane wind loads has also been updated (NRC, 2011). These changes in the calculations of the wind load have resulted in a lower design wind load. Currently the Structural Engineering Institute (SEI) of ASCE is discussing the impacts of climate change on building codes including wind loads and snow loads. These impacts are expected to be incorporated into ASCE 7-28 at the earliest.

The basis for calculating snow loads in the Eurocode was provided by Sanpaolesi et al. (1998). The second-generation Eurocode is expected to provide a harmonized snow load map for the entire EU updated with more recent meteorological observations. The wind section was developed using research by the ECCS, Cook (1990) and Dyrbye and Hansen (1997). Aside from harmonizing the wind load maps, and including regional updates with more recent data (e.g., Figure 2-3), other proposed updates of the wind section do not concern the statistical formulation but only the aerodynamic models of wind behavior (Hansen, 2019). Discussions on how to incorporate climate change have started at least as early as 2015 for the Eurocode. Methods for incorpo-

rating climate change into snow loads have also been proposed in research by Croce, Formichi and Landi (2020), but its applications are also currently being discussed.



WZ	I	II	III	IV	V
vref [m/s]	22.5	25.0	27.5	30.0	32.5

Figure 2-3: Proposal for new wind load maps for Germany (Fig. 10. from Kasperski, 2002)

Societal risk criteria are often used alongside design codes. The development of societal risk criteria started to become more popular in the 1980s. The ALARP principle (as low as reasonably practicable) was also published during this time in the UK (HSE,

1988). At the same time, the use of FN curves, which are in principle a type of frequency-consequence curve, in combination with the ALARP principle also gained popularity in many risk applications (see Figure 2-4). Many countries also started to set annual individual mortality risk criteria in the context of societal risk frameworks along with these other developments. Together, these developments formed the basis of national or regional risk criteria over the years. The Australian states of New South Wales and Western Australia adopted annual individual mortality risk criteria in the context of industrial hazards and land use planning to 0.5×10^{-6} – 100×10^{-6} (EPA WA, 1987; Department of Planning NSW, 1992). The Netherlands also published regulations setting annual individual mortality risk criteria of 10^{-6} for many applications (VROM, 2004). Other organizations also adopted target structural reliability levels that translate to an annual risk of fatality on the order of 10^{-6} , including ISO 2394:2015 (ISO 2015) and Eurocode EN1990:2002 (CEN 2002). U.S. government agencies such as the Nuclear Regulatory Commission (NRC), the Department of Energy (DOE), the Environmental Protection Agency (EPA), and the Occupational Safety and Health Administration (OSHA) all use varying degrees of individual mortality risk-based on the context of the application (NRC, 1995; DOE, 1991; Rhomberg, 1997). Guidelines for societal risk due to dam failures were also published in Australia (ANCOLD, 1998). In the UK, guidelines for risk in the transport sector were published in 1991 (HSE, 1991). Hong Kong published societal risk criteria in 1993 after many years of development from landslide risk applications (Planning Dept. HK, 1993). In recent years, research has also extended these societal risk concepts to other engineering applications such as earthquake engineering (Crowley et al., 2012; Liel and Deierlein, 2012; Tanner and Hingorani, 2015; Tsang et al., 2020).

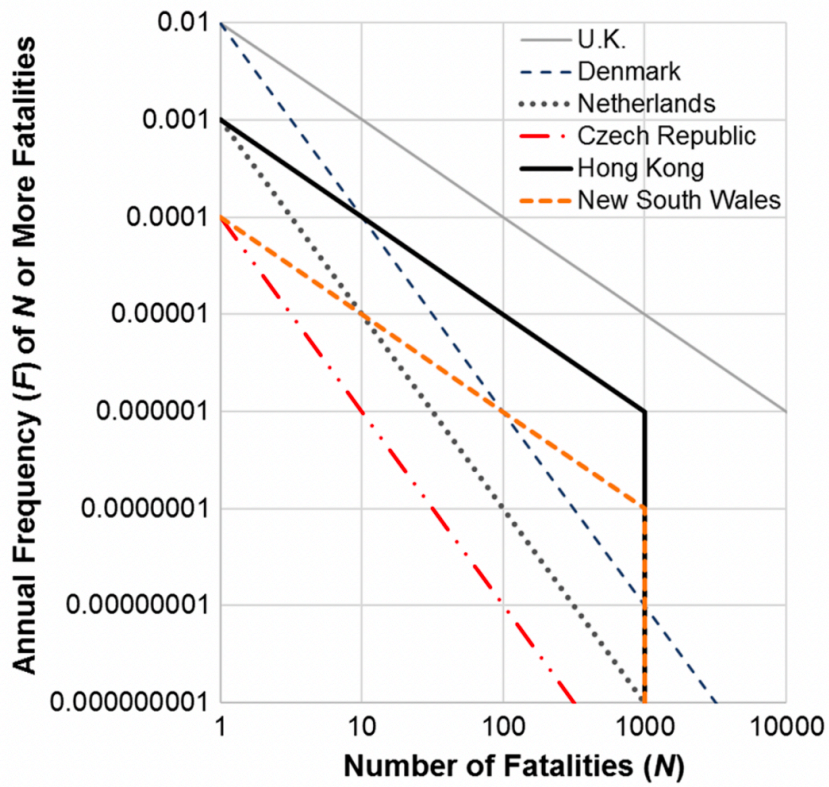


Figure 2-4: FN curves of the upper bound of ALARP region from various standards and guidelines (Fig. 7 from Tsang et al., 2020)

3. Method

The formulation of a risk-based design criteria is composed of a resistance (or demand) component and a load component. The design equation states that the load must not exceed the resistance, otherwise, the design is considered unacceptable:

$$UHII_{design} \geq UHII_{50} \quad (3.1)$$

This framework was demonstrated for a case study area in Kempten, Germany. This section outlines the details of the methodology.

3.1. Study Area

The study area is a residential district of Kempten, Germany of approximately seven hectares with a proposal of two new residential buildings. Kempten is located in the southwest region of the German state of Bavaria near the Alps. The geographical categorization of Kempten is D66 – pre-alpine marsh and hill country and 035 – Iller foothills (Meynen et al., 1962). This region has a temperate climate (Köppen climate classification temperate oceanic climate), and residential buildings typically are not air-conditioned. The long-term (1991-2020) mean annual air temperature of Kempten is 8.2 °C and the hottest month is July with a mean air temperature of 17.4 °C (DWD, 2022). The municipal district where the study area is located has a population density of 5130 inhabitants per square kilometer (1050 total inhabitants) with 15.6% of the inhabitants over 65 years old, 78% between the ages of 15 and 65, and 6.4% under 15 years old and a gender split of 54% male to 46% female (City of Kempten, 2021). The following methodology was developed for southern Germany (Baden-Württemberg and Bavaria) and analyzed locally for the study area. The grouping of climatological regions together is consistent with the methodologies of other environmental load effects in design codes (ASCE, 2017; CEN, 2003).

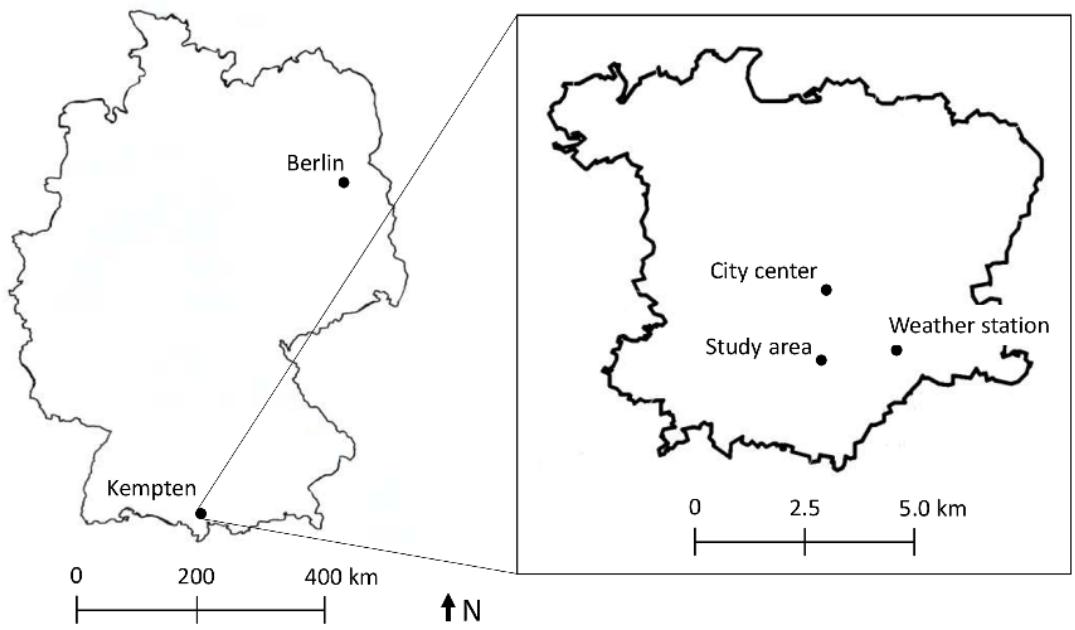


Figure 3-1: Map of study area



Figure 3-2: Satellite image of study area (Google Maps)

3.2. Meteorological Data

Hourly meteorological data (1955-2021) was obtained from the German Weather Service (DWD). The weather station from which the data was obtained was located in the rural outskirts of Kempten. From the DWD dataset, the annual hottest week was derived from the highest rolling seven-day mean of the hourly air temperatures at two meters, *tas*, and used in the statistical analysis (all temperatures and UHI were based on hottest week temperatures so *HW* subscripts for all variables have been dropped for clarity).

Hourly meteorological data from the National Oceanic and Atmospheric Administration's (NOAA) Integrated Surface Dataset (ISD) were used for UHI modelling. The data from NOAA are a collection of data from databases all over the world and are of the ISD file format. The NOAA dataset was used because the modelling tool can only convert ISD files to EPW files. The conversion process was necessary because the modelling process requires EPW files as input. The dataset from NOAA only had complete data from 1973-1992. After the conversion to the EPW file format, any year with outliers in two or more consecutive hours in the horizontal infrared radiation intensity in the period of June to August was excluded. Only the data from 1990 was excluded in this step. This step was necessary because the UHI simulations in subsequent steps did not run if there were too many outliers in the horizontal infrared radiation intensities.

3.3. Mortality Data

Mortality data from the Bavarian State Office for Statistics and Data Processing was used to establish a regional exposure-response relationship for temperature and mortality in a study by Breitner et al. (2014). This mortality data was not directly used in this study due to data protection laws but published values based on the data were available which could be interpolated for this paper. The interpolated values were confirmed with a separate study by an der Heiden et al., (2019) using data from the Federal Statistical Office of Germany (Destatis). Monthly mortality data (June-August) of Baden-Württemberg and Bavaria from 1990-2019 from Destatis was used to estimate the regional mean weekly mortality. Only the period from June to August were considered since the annual hottest weeks occurred during this period. [Section 3.4.3](#) outlines in detail how this mortality data was used to determine the resistance.

3.4. Resistance

The resistance is defined as the allowable urban heat island intensity, $UHII_{design}$. The resistance was determined regionally for southern Germany (Baden-Württemberg and Bavaria). There were three main steps in determining the resistance. The development of this side of the design equation is summarized on the left side of Figure 3-5.

3.4.1. FN Curves

The purpose of using FN curves was to incorporate societal risk into the design framework. FN curves are commonly used in other similar societal risk applications (Tsang et al., 2020). FN curves describe frequency-consequence relationships, which in the context of this paper was the frequency of an annual hottest week (F) and the heat-related mortality (N). The construction of the curves was based on equations of the following form with parameters b and k that describe the level of risk:

$$F * N^b = k \quad (3.2)$$

Typical parameters adopted by regulatory authorities in similar societal risk context were used, and the curve was plotted on a log-log scale. Based on equation 3.2, if $a = \log(k)$ was defined, the generalized form of the upper bound of the FN curve became:

$$\log(F_{BU}) = a - b * \log(N) \quad (3.3)$$

The FN curve was then scaled based on the population of southern Germany according to the methodology and equations presented by Tsang et al. (2020):

$$PLL_{BU} = \sum_{N=1}^{N_{B,max}} F_{BU}(N) \quad (3.4)$$

$$\theta_p = \frac{P * \lambda_{D,tolerable}}{PLL_{BU}} \quad (3.5)$$

$$\log(F_{PU}) = a - b * \log(N) + \log(\theta_p) \quad (3.6)$$

PLL_{BU} is the annual potential loss of life. This was used to calculate the population scaling factor, θ_p , where P is the population of the target area and $\lambda_{D, \text{tolerable}}$ is the tolerable annual individual risk of fatality. Scaling equation 3.3 by θ_p yields equation 3.6. The scaling factor was applied for the population of southern Germany at the reference year, 2003, because the research that determined the temperature-mortality relationship was centered around the heatwave from 2003. The 50-year return period was used as the reference frequency, which is also consistently used in other building design applications. From the reference frequency, the tolerable number of deaths, $N_{\text{tolerable}}$, was obtained directly from the curve.

3.4.2. Statistical Analysis

The goal in this step is to obtain the 50-year hottest week, tas_{50} for southern Germany (Bavaria and Baden-Württemberg). This is the highest seven-day mean for air temperature in a year that statistically is exceeded once every 50 years, also known as the 50-year return period.

The annual hottest week (highest seven-day rolling mean of daily mean temperatures in a year), tas , was used for our analysis as it has been shown to be well correlated to heat-related mortality for southern Germany (an der Heiden et al., 2019). This is likely because heat mortality is usually not caused by a short-term temperature spike but by higher temperatures sustained over several days. Also, other indicators may describe thermal comfort better, but when people start to adapt to the temperature such as taking shelter from the heat, air temperature becomes more influential in describing heat mortality. Whether a shorter- or longer-term temperature mean would have been even more accurate than an der Heiden et al.'s (2019) proposal of a seven-day temperature mean was not investigated in this study.

The generalized extreme value (GEV) probability distribution was used to model the meteorological data. The GEV has been proven to be a good fit to model annual extreme temperatures (Garcia-Cueto et al., 2021; Supian and Hasan, 2021; Tanarhte, Hadjinicolaou and Lelieveld, 2015; Twumasi-Ankrah and Nyantakyi, 2019) and was also extended to annual extreme multi-day temperature averages (Yiou, 2020). For the study area, statistical tests in MATLAB using the Akaike information criterion (AIC) and the log likelihood (LL) of the annual hottest weeks also confirmed that the GEV distri-

bution was the best probability distribution to describe the data. The parameters of the distribution were estimated using maximum likelihood estimation (MLE).

Since the resistance component required only statistical analysis of rural temperatures as input, it was possible to directly use the longer meteorological dataset from DWD (in contrast, the UHI modelling step required the NOAA dataset). To obtain tas_{50} , the population-weighted annual hottest week values of 1955-2021 for southern Germany was first calculated. The values were weighted based on the population of governmental districts and the tas from a representative weather station for each district. Representative weather stations were primarily chosen based on data availability and secondarily based on distance to the centroid of the district. The locations of the weather stations are shown in Figure 3-3. This method was reasonable since the variation of temperatures within governmental district was negligible. The result was one tas value for southern Germany for each year from 1955-2021.

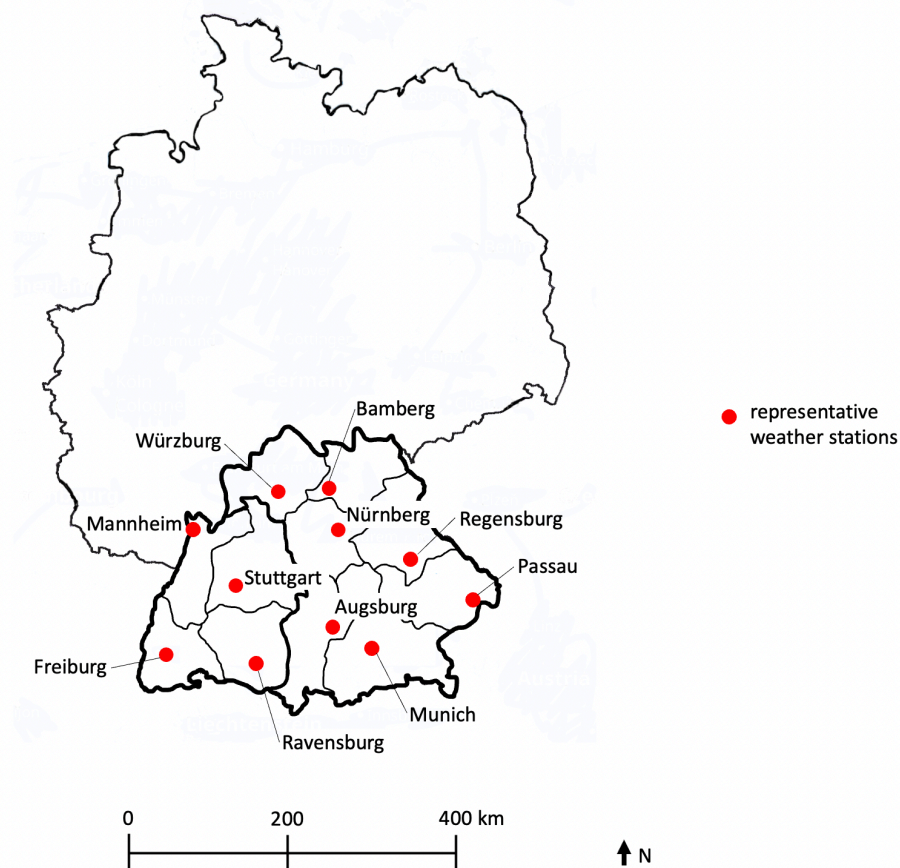


Figure 3-3: Location of representative weather stations by governmental districts

The annual maximum approach was used to determine tas_{50} based on the regional tas . With the GEV distribution, tas_{50} was obtained with confidence intervals, which were also expressed as exceedance probability curves. The analysis was done using custom MATLAB scripts. The overall statistical approach to determine the 50-year hot-test week values is consistent with the statistical approaches from other civil engineering applications.

3.4.3. Exposure-Response

In principle, the temperature-mortality relationship should be determined at tas_{50} from [section 3.4.2](#) since the temperature-mortality curve is non-linear for southern Germany (Figure 3-4).

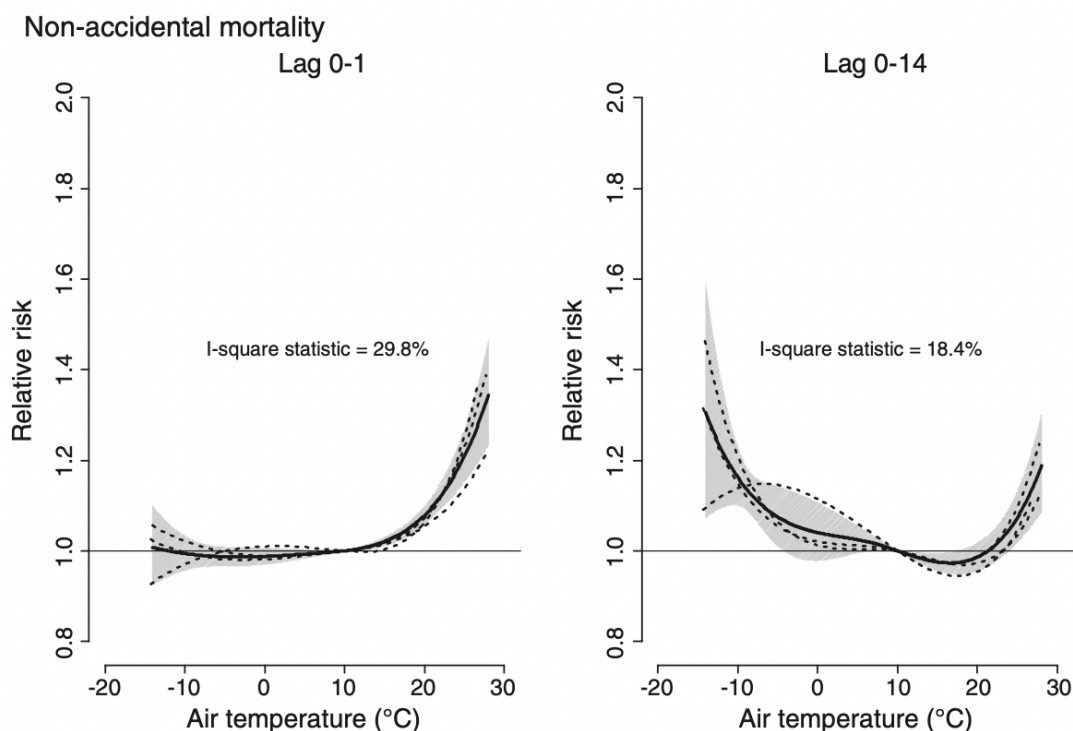


Figure 3-4: Excess heat-mortality exposure-response curve for Bavaria (Fig. 1 from Breitner et al., 2014)

However, the temperature-mortality equations and data in this case were not accessible due to data protection laws. Therefore, tas_{50} was not used. Instead, an interpolation of published values of temperature-mortality relationship from Breitner et al.'s (2014) research was used. In consultation with the author, this relationship was adapted by interpolating the two-day values and the 15-day values to obtain the relative risk of heat-related deaths per degree Celsius increase over a seven-day period.

This value also corresponded closely to the values derived from Destatis by an der Heiden et al. (2019) for southern Germany. This value was multiplied by the mean weekly mortality (see [section 3.3](#)) to obtain the number of heat-related deaths per degree Celsius over a seven-day period. This value was then used to divide $N_{tolerable}$ from [section 3.4.1](#) to obtain the allowable increase in temperature due to UHI, UHI_{design} . The benefit of directly utilizing local or regional temperature mortality relationships is that the differences in the heat adaptability of populations are automatically accounted for.

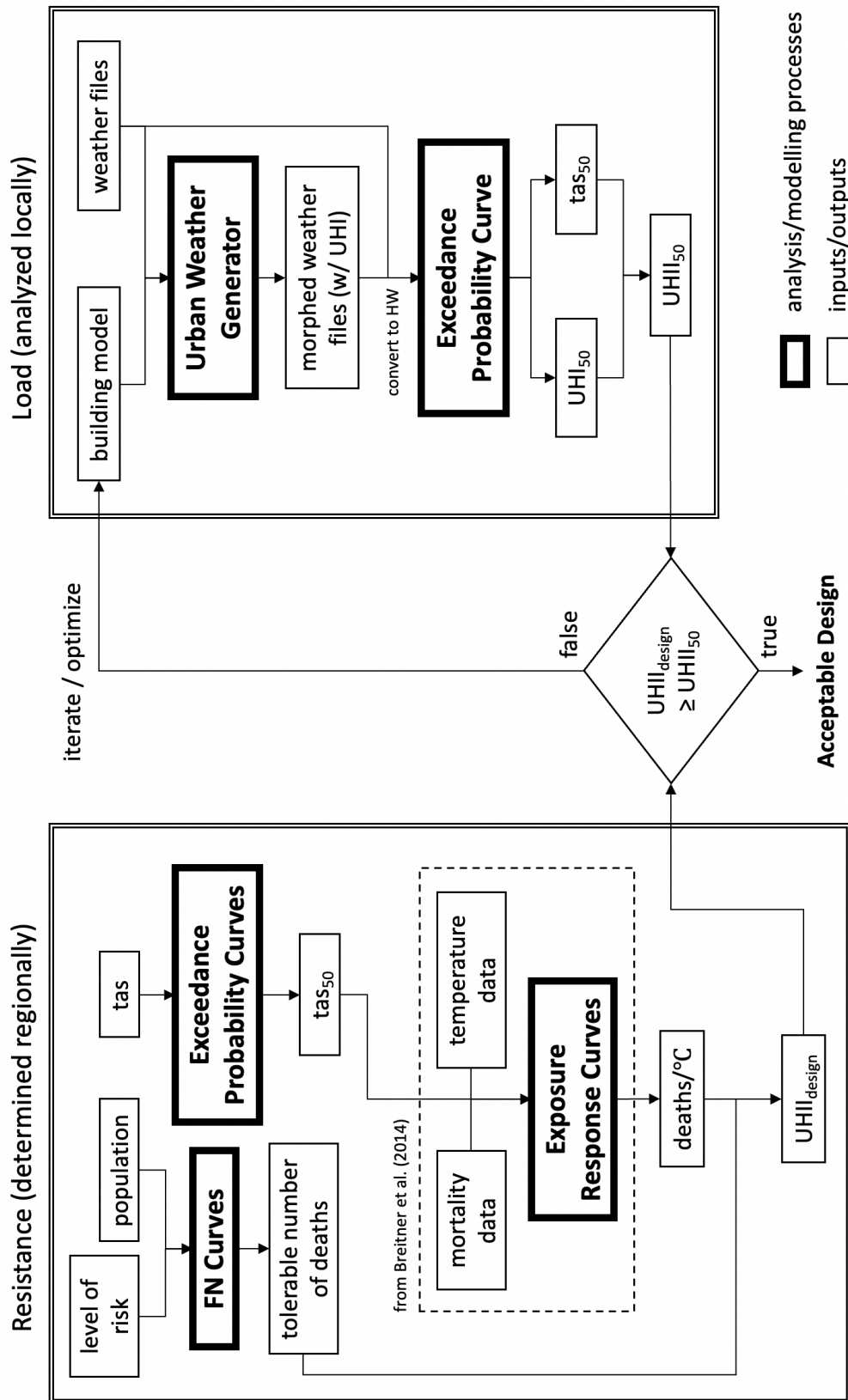


Figure 3-5: Risk-based framework for developing UHI design criteria

3.5. Load

Whereas the resistance was determined regionally, the load was determined locally for Kempten, Germany. The load is defined as the local 50-year UHII of the area under consideration, $UHII_{50}$. The load side of the design equation is summarized on the right side of Figure 3-5.

3.5.1. UHI Modelling

The Urban Weather Generator (UWG) was used for the UHI modelling. UWG is a Python application in the Ladybug tools plug-in for Rhinoceros 3D, a computer-aided design software (Roudsari, Pak, and Smith, 2013). UWG is a computationally more efficient model than some other UHI modelling tools and uses energy balance principles to calculate urban air temperature and humidity from rural weather data (Bueno et al., 2013). Modelling tools such as the UWG are necessary because weather stations are often located in more rural areas. As a result, UHI cannot be measured directly in many cases. The modelling process with UWG requires EPW files for the weather data input and a 3DM file for the building model. The EPW files were obtained by converting the NOAA ISD files and the 3DM file of the study area was provided by the Institute of Energy Efficient and Sustainable Design and Building at TUM.

The UWG has 50 input parameters and the most significant parameters for UHI have been identified through many sensitivity studies (Banhashemi, Reitberger and Lang, 2022, Ibrahim et al. 2021, Nakano et al., 2015, and Salvati, Massimo and Inostroza, 2017). The input parameters of the study area have also been provided by the Institute of Energy Efficient and Sustainable Design and Building and are listed in Table 3-1. Among the most significant parameters, only the building footprint density, the façade-to-site ratio (vertical to horizontal urban area ratio) and tree coverage were analyzed in the design framework in order to focus on the risk aspects of the framework. The output of the modelling process was in the form of morphed urban EPW files (1973-1992, excluding 1990) that accounted for UHI. Then, the hottest week values were calculated for the morphed urban EPW files (UHI) and the original EPW files (tas) for the statistical analysis. Both UHI and tas were necessary because the goal was to obtain $UHII$ in the next step. $UHII$ values are more easily evaluated in the design equation.

Table 3-1: Description of input parameters for UHI modelling

Parameter	Value	Description
albroad	0.16	Average road albedo
albroof	0.29	Average building roof albedo
albveg	0.25	Average vegetation albedo
albwall	0.16	Average building wall albedo
autosize	false	Boolean to auto size HVAC system
bld	[('midriseapartment', 'pre80', 0.97), ('secondarieschool', 'pst80', 0.03), ('warehouse', 'pre80', 0.005)]	Matrix representing fraction of urban building stock
blddensity	[0.3, 0.5, 0.75]	Building footprint density as fraction of urban area
bldheight	13.9 m	Average building height
c_circ	1.2	Wind scaling coefficient
c_exch	1.0	Exchange velocity coefficient
charlength	258.0 m	Urban characteristic length
croad	1600000.0 J/m ³ K	Road pavement volumetric heat capacity
droad	0.5 m	Thickness of road pavement
flr_h	3.15 m	Average building floor height
glzr	0.25	Glazing ratio/WWR
grasscover	0.1	Fraction of urban area covered by grass
h_mix	1.0	Fraction of building HVAC waste heat released to street canyon
h_obs	13.0 m	Rural obstacle height
h_ref	150.0 m	Inversion height
h_temp	2.0 m	Height of rural temperature measurement
h_ubl1	1000.0 m	Daytime urban boundary layer height
h_ubl2	80.0 m	Nighttime urban boundary layer height
h_wind	10.0 m	Wind height
kroad	1.0 W/mK	Road pavement conductivity
latfocc	0.3	Latent heat fraction from occupant
latgrass	0.5	Fraction of latent heat absorbed by grass
lattree	0.7	Fraction of latent heat absorbed by trees
maxday	150 W/m ²	Maximum heat flux threshold for daytime conditions
maxnight	20 W/m ²	Maximum heat flux threshold for nighttime conditions
nday	122	Number of days for simulation
radfequip	0.5	Fraction of radiation heat fraction from equipment
radflight	0.7	Fraction of radiant heat from electric light
radfocc	0.2	Fraction of radiant heat from occupant
ruvegcover	0.5	Fraction of rural ground covered by trees and grass
schtraffic	(0.03, 0.03, 0.03 0.02 0.03 0.03, 0.06, 0.10, 0.10, 0.90, 0.90, 0.10, 0.10, 0.11, 0.11, 0.11, 0.12, 0.11, 0.09, 0.07, 0.06, 0.05, 0.05, 0.04, 0.04)	Traffic schedule
sensanth	11.76 W/m ²	Street level anthropogenic heat
sensocc	100 W	Sensible heat gain from occupant
shgc	0.42	Building glazing solar heat gain coefficient
treecover	[0.1, 0.5]	Fraction of urban ground covered in trees
vegend	10	Month in which vegetation stops evapotranspiration
vegroof	0.0	Fraction of roof covered in vegetation
vegstart	5	Month in which vegetation starts evapotranspiration
vertohor	[0.8, 1.5, 2.0]	Vertical to horizontal urban area ratio
windmin	1 m/s	Minimum wind speed
zone	5C	Climate zone in which area exists

3.5.2. Statistical Analysis

The statistical analysis in this section followed the same approach as [section 3.4.2](#). tas was taken from 1973-1992 (excluding 1990) of the NOAA dataset to fit the GEV distribution because the UHI modelling process required the NOAA dataset due to the EPW file conversion process (see [section 3.2](#) and [section 3.5.1](#)). UHI and tas were taken from consistent data sources to prevent inconsistencies in the analysis. The statistical analysis yielded UHI_{50} and tas_{50} . $UHII_{50}$ was obtained from equation 3.7:

$$UHII_{50} = UHI_{50} - tas_{50} \quad (3.7)$$

4. Results

On the resistance side, the range of variables used for the FN curves and the resulting $N_{tolerable}$ are summarized in Table 4-1. A value of $b = 1.0$ indicates risk neutrality whereas $b = 2.0$ indicates risk aversion. The annual individual risk of fatality, $\lambda_{D,tolerable}$, is taken as 10^{-6} in many practical applications although 10^{-5} is also used by some authorities. $N_{r,max}$ of 0.03% of the population was used as the base value since that number reflects the ratio of intensive care unit beds to the total population for southern Germany (Destatis, 2020). The actual percentage would be lower since a portion of the intensive care unit beds would be occupied for other reasons. A total population, P , of 23,115,942 (2003) was used for the scaling factor, θ_p , to construct the FN curves. The FN curve for the case where $\lambda_{D,tolerable} = 10^{-6}$, $b = 2.0$, and $N_{r,max} = 0.0003P$ is plotted in Figure 4-1.

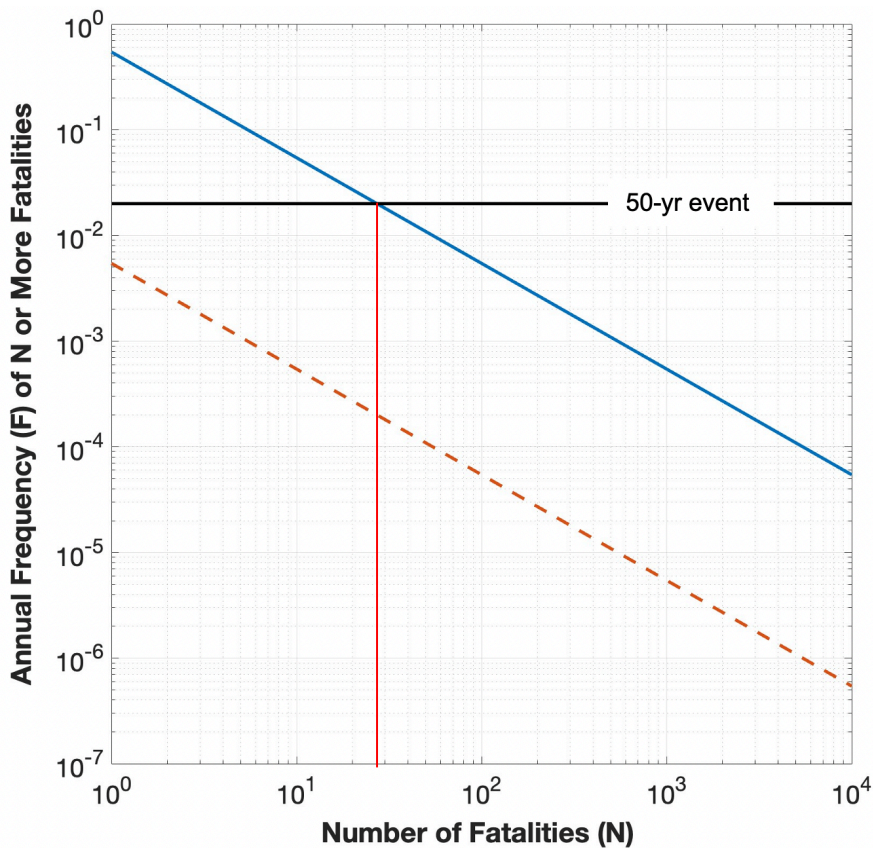


Figure 4-1: Population adjusted FN curve for southern Germany ($\lambda_{D,tolerable} = 10^{-6}$, $N_{R,max} = 0.0003P$ & $b=2.0$)

Table 4-1: $N_{tolerable}$ based on a range of risk parameters

(a) $\lambda_{D,tolerable} = 10^{-5}$			
	$b = 1.0$	$b = 1.5$	$b = 2.0$
$N_{R,max} = 0.0003P$	1227	271	84
$N_{R,max} = 0.001P$	1088	270	84
$N_{R,max} = 0.005P$	945	270	84
(b) $\lambda_{D,tolerable} = 10^{-6}$			
	$b = 1.0$	$b = 1.5$	$b = 2.0$
$N_{R,max} = 0.0003P$	123	58	27
$N_{R,max} = 0.001P$	109	58	27
$N_{R,max} = 0.005P$	94	58	26

The published temperature-mortality relationship for Bavaria was a 11.4% (95% CI: 7.6-15.3) increase of relative risk over a 4.8 °C increase for a two-day lag and a 8.2% (95% CI: 4.6-12.1) increase for a 15-day lag (Breitner et al., 2014). By interpolation, the increase in relative risk for seven-day lag was 2.1%/°C (95% CI: 1.3-2.9). From temperature-mortality graphs in an der Heiden et al.'s (2019) research, the value for southern Germany was approximately an increase of 2.5%/°C by inspection, which is reasonably consistent with the value from Breitner et al., (2014). The regional mean weekly mortality was 4400 for southern Germany (Destatis). An increase of 2.1%/°C (95% CI: 1.3-2.9) was used for the excess heat mortality risk increase to multiply the weekly mortality for southern Germany. This yielded an excess heat mortality rate of 93 deaths/°C (95% CI: 57 deaths/°C - 128 deaths/°C). Dividing the $N_{tolerable}$ from Table 4-1 by the excess heat mortality rate yielded $UHII_{design}$ which is presented in Table 4-2. These are the resistance values for the design equation.

Table 4-2: $UHII_{design}$ in Celsius based on a range of risk parameters

(a) $\lambda_{D,tolerable} = 10^{-5}$			
	$b = 1.0$	$b = 1.5$	$b = 2.0$
$N_{R,max} = 0.0003P$	13.2° (9.6°-21.5°)	2.9° (2.1°-4.8°)	0.9° (0.7°-1.5°)
$N_{R,max} = 0.001P$	11.7° (8.5°-19.0°)	2.9° (2.1°-4.7°)	0.9° (0.7°-1.5°)
$N_{R,max} = 0.005P$	10.2° (7.4°-16.6°)	2.9° (2.1°-4.7°)	0.9° (0.7°-1.5°)
(b) $\lambda_{D,tolerable} = 10^{-6}$			
	$b = 1.0$	$b = 1.5$	$b = 2.0$
$N_{R,max} = 0.0003P$	1.3° (1.0°-2.2°)	0.6° (0.5°-1.0°)	0.3° (0.2°-0.5°)
$N_{R,max} = 0.001P$	1.2° (0.8°-1.9°)	0.6° (0.5°-1.0°)	0.3° (0.2°-0.5°)
$N_{R,max} = 0.005P$	1.0° (0.7°-1.7°)	0.6° (0.5°-1.0°)	0.3° (0.2°-0.5°)

On the load side, the building model and input modelling parameters of the study area for the UHI modelling were provided by the Institute of Energy Efficient and Sustainable Design and Building and 19 years of annual hottest week UHI temperatures were calculated from the weather files from NOAA. As previously mentioned, the year 1990 was excluded due to the occurrence of too many outliers in the horizontal infrared radiation intensity. For UHI, the statistical analysis yielded an $UHI_{tot,50}$ of 23.56 °C. The statistical analysis of the NOAA data without UHI, yielded a tas_{50} of 23.39 °C (95% CI: 20.98 °C – 28.76 °C). Subtracting tas_{50} from $UHI_{tot,50}$ yielded an $UHII_{tot,50}$ of 0.17 °C (see Figures 4-2 and 4-3). Scenarios with and without the proposed development were analyzed to also determine the contribution to $UHII_{tot,50}$ from only the proposed development. The UHII caused by the proposed development, $UHII_{new,50}$, was 0.04 °C. The UHII caused by existing conditions, $UHII_{existing,50}$, was 0.13 °C. Confidence intervals for the UHI values were not calculated because although the statistical uncertainties were calculated, the UWG model uncertainties and model input uncertainties were not known. A separate more rigorous uncertainty assessment should be conducted to provide information on the model and input uncertainties. Figure 4-2 only presents the confidence intervals due to statistical uncertainties. Several scenarios for a range of values of façade-to-site ratio, building footprint density, and tree coverage percentage were also analyzed for reference. The values of $UHII_{50}$ are presented in Table 4-3.

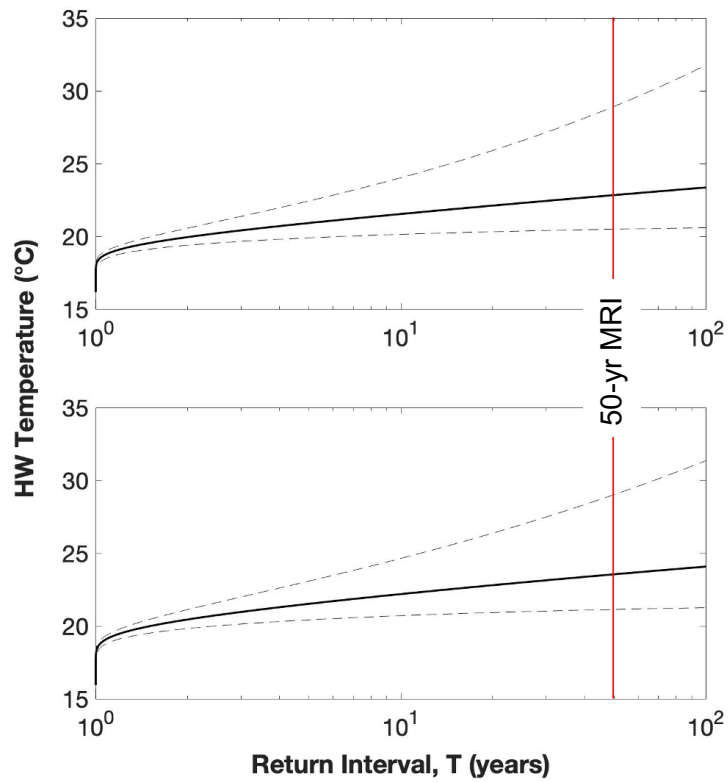


Figure 4-2: Exceedance probability curves with 95% confidence intervals of *tas* (top) & *UHI_{tot}* of the study area (bottom)

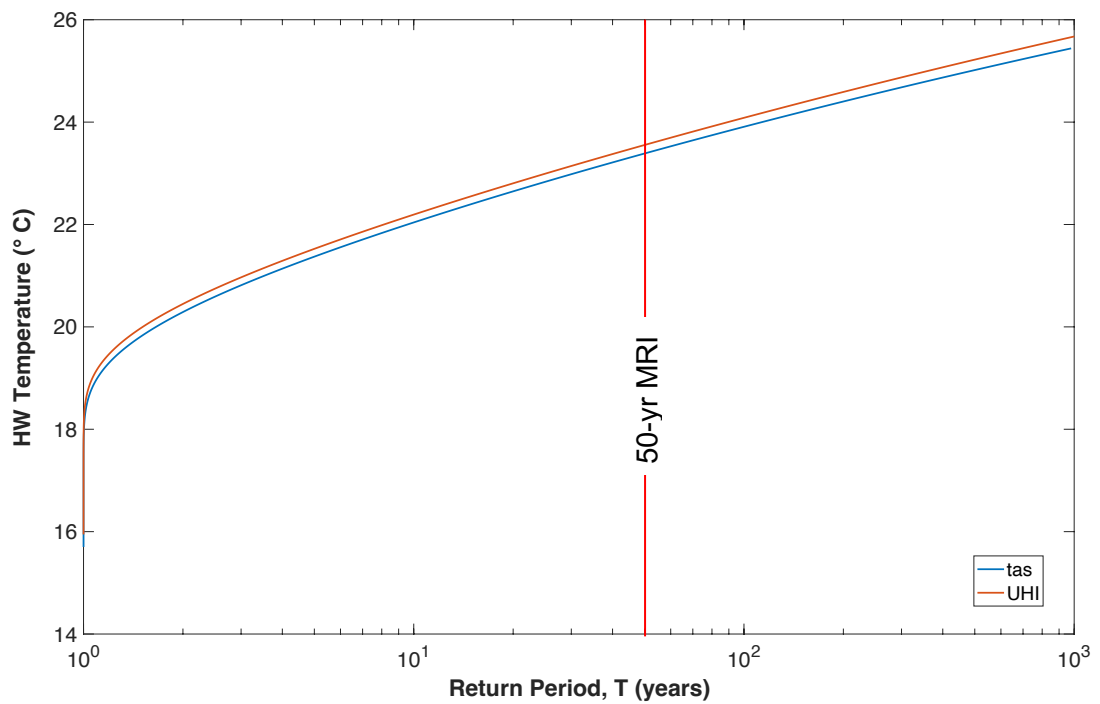


Figure 4-3: Exceedance probability curves of *tas* & *UHI_{tot}* of the study area

Table 4-3: $UHII_{50}$ in Celsius based on different scenarios of tree cover, footprint density, and façade-to-site ratio; $UHII_{tot,50}$ and $UHII_{new,50}$ for the study area are in bold

(a) Tree Coverage = 10%			
Footprint Density %	Façade to Site Ratio		
	0.8	1.5	2.0
30%	0.17° (0.04°)	0.21°	0.22°
50%	0.22°	0.27°	0.30°
75%	0.36°	0.44°	0.48°

(b) Tree Coverage = 50%			
Footprint Density %	Façade to Site Ratio		
	0.8	1.5	2.0
30%	0.16°	0.20°	0.22°
50%	0.22°	0.27°	0.30°
75%	0.36°	0.44°	0.48°

5. Discussion

5.1. Resistance

On the resistance side, a range of $UHII_{design}$ were presented in Table 4-2 that are based on parameters used in practice in other risk applications. The uncertainty in the $UHII_{design}$ values is non-trivial and should be taken into account through scaling factors. Determining these factors are also non-trivial and should be addressed in future research. Once appropriate resistance factors are determined, it is up to the decision maker to decide upon an appropriate value for the given region in which the criteria are applied. This may be based on decision analysis tools such as cost-benefit analysis to weight the costs of adopting more risk averse values against the benefits of mitigating UHI. It is recommended that the more risk seeking, and risk neutral scenarios be avoided. From Table 4-2, it can be seen that scenarios with $\lambda_{D,tolerable} = 10^{-5}$ with $b = 1.0$ and 1.5 have a $UHII_{design}$ (2.9 °C – 13.2 °C) that are currently met by most urban areas by a wide margin. When it comes to public safety and buildings, $\lambda_{D,tolerable}$ values on the order of 10^{-6} , are typically used (CEN, 2002; ISO, 2015). Scenarios with $\lambda_{D,tolerable} = 10^{-6}$ have a $UHII_{design}$ of 0.3 °C - 1.3 °C and represent a more acceptable target for UHI mitigation. For urban areas in which the existing conditions do not meet a selected design criteria, having a two-tier design criteria for new developments and existing conditions can be considered. This has also been used in other engineering applications where new developments are subject to stricter criteria.

5.2. Load

Regarding the rural air temperatures, the relatively small sample size of 19 years of the NOAA dataset (1973-1992 excluding 1990) caused higher uncertainty in tas_{50} . For reference, the tas_{50} from the DWD dataset which covered 1952-2021, was 24.06 °C (95% CI: 21.89 °C – 28.14 °C). This was considerably higher with less uncertainty than the tas_{50} of 23.39 °C (95% CI: 20.98 °C – 28.76 °C) from the NOAA dataset. This higher tas_{50} from the DWD dataset was due to several hot years in the 21st century that were not included in the NOAA dataset ($tas_{2003} = 23.27$ °C, $tas_{2006} = 22.81$ °C, $tas_{2010} = 22.69$ °C, $tas_{2015} = 23.99$ °C, $tas_{2018} = 23.11$ °C and $tas_{2019} = 23.74$ °C). However, it is uncertain whether a higher tas_{50} is related to a higher $UHII_{50}$. Research has observed

cases of both higher air temperatures causing higher UHI (Founda and Santamouris, 2017 and Zhao et al., 2018) and higher air temperatures having insignificant effects on UHI (Chew et al., 2021 and Richard et al., 2021). Nevertheless, the NOAA data was the only data set available that could be converted to EPW files for the UHI modelling, and the uncertainty of its t_{as50} has been defined through confidence intervals.

Regarding the $UHII_{50}$ values, they were noticeably lower than typical values of UHI because the annual hottest week temperatures were used. Also, the study area was relatively less dense compared to other areas. For reference, urban densities of five residential districts from other UHI studies (Bueno et al., 2013 and 2014 and Salvati, Massimo and Inostroza, 2017) are shown in Figure 5-1. An interesting topic of future research would be to evaluate denser urban areas with this UHI design criteria.

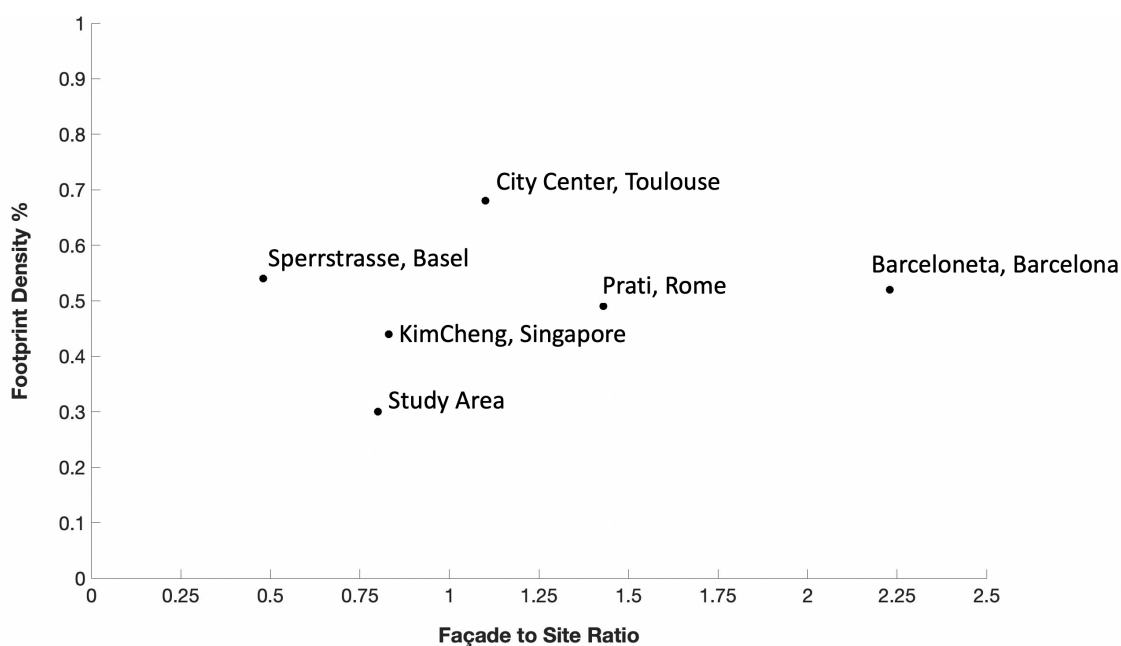


Figure 5-1: Plot of reference residential districts and their urban density parameters

Another observation is that the tree coverage had a minimal impact on the load. This is consistent with other studies which mention that tree coverage is more influential on mean radiant temperature and thermal comfort compared to air temperature (Heris, Middel and Muller, 2020, Kamal et al., 2021, Salvati, Massimo and Inostroza, 2017). When averaged across daytime and nighttime air temperatures for hottest week calculations, the cooling effects of tree coverage are even less. This is because the cooling effect of trees are greatest during the hottest parts of the day and less during nighttime (Chen, Jin and Du, 2020). The maximum increase in $UHII_{50}$ across all scenarios was

0.01 °C for an increase in tree coverage from 10% to 50%. This occurred at the lower urban densities (footprint density of 30% and façade-to-site ratio of 80% and 150%). Therefore, although trees have a cooling effect experienced in the form of thermal comfort and directly under the tree canopy, their effect on the hottest week temperatures and indirectly on the excess heat mortality is shown to be limited.

5.3. Practical Application

Comparing the $UHII_{tot,50}$ of 0.17 °C from the study area with $UHII_{design}$ from Table 4-2 shows that the study area does not exceed the design criteria for all risk scenarios. This was not surprising, given that the urban density of the study area was relatively low. However, the UHII due to the proposed development, $UHII_{new,50}$, was 0.04 °C which is approximately a 33% increase from the $UHII_{existing,50}$. This seemed to indicate that the study area is relatively sensitive to densification and could easily approach the lower confidence interval of $UHII_{design}$ if for example, the proposed development were to be taller or larger than expected, the sensible anthropogenic heat increases due to more traffic, or other unforeseen changes.

The choice of risk parameters specifically for southern Germany is non-trivial. For the region of southern Germany, a choice of $N_{R,max} = 0.0003P$ is logical, using the maximum capacity of intensive care unit beds as a benchmark (Destatis, 2020). $\lambda_{D,tolerable} = 10^{-6}$ is mainly used when considering risk to the general public and is used by many building codes and standards. However, the choice of $b = 1.0$ (risk neutral) to $b = 2.0$ (risk averse) with $UHII_{design}$ values of 0.3 °C – 1.3 °C is not trivial. For reference, Germany adopted a value of $b = 2.0$ for road tunnel safety (Spouge, Skjong and Olufsen, 2015) which may indicate a national preference for risk averseness. If southern Germany were to adopt $b = 2.0$ in this case, the corresponding $UHII_{design}$ of 0.3 °C would not be exceeded by the study area. However, other denser cities in the region like Munich could approach or exceed this design criteria. Even other parts of Kempten are considerably denser and may be in danger of exceeding $UHII_{design}$. Therefore, under the scenario where $b = 2.0$, significant changes to the urban morphology may be needed in the densest urban areas, which can quickly become cost prohibitive. $b = 1.0$ or $b = 1.5$ may be a more realistic scenario when considering southern Germany as a whole. As mentioned previously, other decision analysis tools such as a cost-benefit analysis should be used to guide the final decision for an optimal $UHII_{design}$.

6. Conclusion

Although there has been an increase of research in the field of UHI within recent decades, this paper identified a research gap in the development of UHI design criteria and has taken the first steps to address this gap. A novel risk-based design criteria for UHI was developed that provided concrete thresholds for UHI values. Based on this, designers can develop concrete UHI values to guide their mitigation measures more precisely. Urban planners can assess UHI in existing urban areas more strategically and new developments can be designed to account for UHI more precisely.

The design criteria was based on statistical methods and societal risk concepts that have been widely used in engineering and design applications for decades. The design criteria was expressed in the form of a design equation where the UHI load should not exceed the UHI resistance. The design criteria accounted for excess heat mortality risk based on published heat-mortality relationships. This design criteria was demonstrated for a case study area in Kempten, Germany. For the UHI resistance, a range of 0.3 °C – 13.2 °C was calculated based on a range of risk parameters that are commonly used in practice. For southern Germany, a UHI resistance of 0.6°C – 1.3 °C for risk parameters $\lambda_{D,tolerable} = 10^{-6}$, $N_{R,max} = 0.0003P$ and $b = 1.0$ or 1.5 seemed to be a realistic choice, based on risk attitudes in other similar applications and the regional situation. For the UHI load, the UHI modelling was done with the UWG, and the study area was shown to have a load of 0.17 °C. Since the study area was not a dense urban area, it is not surprising that it did not exceed any of the UHI resistance values.

The upper extremes of the range of UHI resistance values presented in this paper represent more risk seeking and risk neutral scenarios and should not be used. Then there is a range of more reasonable resistance values, and it is up to the decision makers and their advisors to use decision analysis tools such as cost-benefit analysis to choose appropriate values for their region. Ultimately, this design criteria was intended to be a design tool that represents the designer's professional responsibility to mitigate excess heat mortality risk due to UHI. Similar to how the safety of a structure or a product is the responsibility of the one who designed it, the heat mortality risk caused by the UHI of an urban area should be the responsibility of those who designed the area. However, an urban area that meets the UHI design equation does not necessarily signify that the overall heat-related risk is acceptable. There are many oth-

er aspects of quantifying and mitigating heat mortality risk that could be considered related to the base rural temperatures or indirectly to UHI for which designers do not have direct control over, such as calibration of heatwave warning systems, implementation methods of educational programs for vulnerable populations, infant safety features in automobiles, and safety protocols for athletics. Therefore, the design criteria developed in this paper should not be misinterpreted for a definitive risk quantification solution for heat mortality risk overall.

The development of the design criteria presented several limitations. Firstly, there were limitations in the availability of heat mortality data. Mortality data is subject to data protection regulations in Germany and obtaining this data requires a license. Furthermore, the accuracy of heat mortality data is a challenge since heat mortality is usually not listed as the cause of death. Typically, the victims have other underlying health conditions which become the primary cause of death. Also, the lack of more weather data in the right file format for the UHI modelling caused higher uncertainties in the tas_{50} and $UHII_{50}$ values. The UWG required EPW files as inputs and finding more years of data in this format for a smaller city like Kempten is often not possible. One solution is to use EPW files from other climatologically similar regions if the data is statistically independent. This would need to be developed in future research. Finally, the temperature-mortality relationship is fundamentally a relatively uncertain process and requires interdisciplinary expertise. Even though, this paper relied on research from leading climatologists and epidemiologists in southern Germany, at a city or even neighborhood scale, the temperature-mortality relationship could vary due to demographics, land use type, quality and availability of health services, heat warning systems, etc.

Heat mortality risk in the context of UHI is a complex and interdisciplinary challenge due to the dynamics and uncertainties of the underlying processes and the wide range of expertise that it touches, and more work is needed in a few main areas to better operationalize a design criteria for UHI. Initially, this design criteria should be tested for other denser urban areas to further validate the methodology. A logical starting point would be to investigate other urban areas in southern Germany. This should include grouping climatologically similar regions together so that there is a larger sample size of weather data for the UHI modelling step. Secondly, more work on simplifying the methodology for practitioners is necessary. This can involve the development of UHI load tables grouped by climatological regions for the most influential urban morpholog-

ical parameters. Designers can then easily look up UHI load values for a particular site based on the site's main urban parameters without the need of their own statistical analysis. Also, scaling factors need to be developed to account for statistical uncertainties, model uncertainties, demographic differences and land use type. The resistance and load values would then be multiplied by these scaling factors for better accuracy and representation of local and regional effects. Finally, with climate change predicted to have a significant influence on extreme temperatures, future work should investigate the impacts of climate change on the UHI design criteria. Preliminary research on incorporating climate change data has already been carried out by the authors but more work still needs to be done on the post processing step before the data can be incorporated.

References

- an der Heiden, M., Muthers, S., Niemann, H., Buchholz, U., Grabenhenrich, L., & Matzarakis, A. (2020). Heat-Related Mortality - An Analysis of the Impact of Heatwaves in Germany Between 1992 and 2017. *Deutsches Arzteblatt*. 117. 603-609.
- an der Heiden, M., Muthers, S., Niemann, H., Buchholz, U., Grabenhenrich, L., & Matzarakis, A. (2019). Schätzung hitzebedingter Todesfälle in Deutschland zwischen 2001 und 2015 [Estimation of heat-related deaths in Germany between 2001 and 2015]. *Bundesgesundheitsbl* 62, 571–579. <https://doi.org/10.1007/s00103-019-02932-y>.
- ASCE/SEI 7-16. (2017). Minimum design loads for buildings and other structures. Reston, VA: American Society of Civil Engineers. <https://doi.org/10.1061/9780784414248>.
- Australian National Committee on Large Dams (ANCOLD) (1998) Guidelines on Risk Assessment, Position Paper on Revised Criteria for Acceptable Risk to Life, August 1998.
- Banihashemi, F., Reitberger, R. & Lang, W. (2022). Investigating Urban Heat Island and Vegetation Effects under the Influence of Climate Change in Early Design Stages. *Proceedings of the 27th International Conference of the Association for Computer-Aided Architectural Design Research in Asia (CAADRIA) 2022, volume 2*, 679-688.
- Barriopedro, D., Fischer, E. M., Luterbacher, J., Trigo, R. M., & García-Herrera, R. (2011). The Hot Summer of 2010: Redrawing the Temperature Record Map of Europe. *Science*, 332 (6026). <https://www.science.org/doi/10.1126/science.1201224>.
- Boé, J., Somot, S., Corre, L. & Nabat, P. (2020). Large discrepancies in summer climate change over Europe as projected by global and regional climate models: causes and consequences. *Clim Dyn* 54, 2981–3002 (2020). <https://doi.org/10.1007/s00382-020-05153-1>.
- Breitner, S., Wolf, K., Devlin, R. B., Diaz-Sanchez, D., Peters, A., & Schneider, A. (2014). Short-term effects of air temperature on mortality and effect modification by air pollution in three cities of Bavaria, Germany: a time-series analysis. *The Science of the total environment*, 485-486, 49–61. <https://doi.org/10.1016/j.scitotenv.2014.03.048>.
- Buska, J. S., Grotorex, A., & Tobiasson, W. (2020). *Site-specific case studies for determining ground snow loads in the United States*. Hanover, NH: U.S. Army Engineer Research and Development Center, Cold Regions Research and Engineering Laboratory (ERDC/CRREL, SR-20-1). <https://doi.org/10.21079/11681/37574>.
- Bueno, B., Roth, M., Norford, L., & Li, R. (2014). Computationally efficient prediction of canopy level urban air temperature at the neighbourhood scale. *Urban Climate*, 9, 35-53. <https://doi.org/10.1016/j.uclim.2014.05.005>.
- Bueno, B., Norford, L., Hidalgo, J., & Pigeon, G. (2013). The urban weather generator. *Journal*

- of *Building Performance Simulation*, 6(4), 269-281.
<https://doi.org/10.1080/19401493.2012.718797>.
- CCFLA (2015). State of City Climate Finance 2015. Cities Climate Finance Leadership Alliance (CCFLA). New York. <https://sustainabledevelopment.un.org/content/documents/2201CCFLA-State-of-City-Climate-Finance-2015.pdf>.
- Chen, J., Jin, S., & Du, P. (2020). Roles of horizontal and vertical tree canopy structure in mitigating daytime and nighttime urban heat island effects. *International Journal of Applied Earth Observation and Geoinformation*, 89, 102060 <https://doi.org/10.1016/j.jag.2020.102060>.
- Chew, L. W., Liu, X., Li, X. X., & Norford, L. K. (2021). Interaction between heat wave and urban heat island: A case study in a tropical coastal city, Singapore. *Atmospheric Research*, 247, 105134. <https://doi.org/10.1016/j.atmosres.2020.105134>.
- City of Kempten. (2021). *Jahresbericht Kempten 2020 [Annual Report Kempten 2020]*. https://www.kempten.de/file/Jahresbericht_Kempten_2020.pdf.
- Cook, N. J. (1990). The designer's guide to wind loading of building structures. Vol. 2: Static structures. *Building Research Establishment Report*.
- Coseo, P., & Larsen, L. (2015). Cooling the heat island in compact urban environments: the effectiveness of Chicago's green alley program. *Procedia Engineering*, 118, 691-710. <https://doi.org/10.1016/j.proeng.2015.08.504>.
- Croce, P., Formichi, P. & Landi, F. (2020). Probabilistic methodology for the assessment of the impact of climate change on structural safety. *Proceedings of the 30th European Safety and Reliability Conference and the 15th Probabilistic Safety Assessment and Management Conference, 1-5 November, 2020, Venice, Italy*.
- Croce, P., Formichi, P., Landi, F. (2019). Climate Change: Impacts on Climatic Actions and Structural Reliability. *Applied Sciences*. 2019; 9(24):5416. <https://doi.org/10.3390/app9245416>.
- Crowley, H., Silva, V., Bal, I. E., & Pinho, R. (2012, September). Calibration of seismic design codes using loss estimation. In *Proceedings of 15th World Conference on Earthquake Engineering, Lisbon, Portugal, Paper (No. 4891)*.
- DWD Climate Data Center (CDC). (2022). *Long-term (1991-2020) mean annual temperatures*. Deutscher Wetterdienst. <http://www.dwd.de>.
- DWD Climate Data Center (CDC). (2022). *Historical hourly station observations of 2m air temperature and humidity for Germany*. Deutscher Wetterdienst. <http://www.dwd.de>.
- Dyrbye, C., & Hansen, S. O. (1997). *Wind loads on structures*. Wiley, Print.
- Ellingwood, B., and Redfield, R. (1983). Ground snow loads for structural design. *J. Struct. Eng.*, 109(4), 950–964. [https://doi.org/10.1061/\(ASCE\)0733-9445\(1983\)109:4\(950\)](https://doi.org/10.1061/(ASCE)0733-9445(1983)109:4(950)).
- Environmental Protection Authority. (1987). *Environmental Protection Regulations 1987*. Perth: EPA.

- European Committee for Standardisation (CEN) (2002). EN 1991-1: Eurocode 1: Basis of Structural Design. Belgium, Brussels.
- European Committee for Standardisation (CEN) (2003), EN 1991-1-3. Eurocode 1: Actions on Structures - Part 1–3: General Actions - Snow Loads, Brussels, Belgium.
- European Committee for Standardisation (CEN) (2005), EN 1991-1-4. Eurocode 1: Actions on Structures - Part 1–4: General Actions – Wind Actions, Brussels, Belgium.
- European Environment Agency. (2022). *Economic losses from weather and climate-related extremes in Europe reached around half a trillion euros over past 40 years*. <https://data.europa.eu/doi/10.2800/530599>.
- Egler, H.-P. & Frazao, R. (2016). Sustainable Infrastructure and Finance: How to Contribute to a Sustainable Future. https://www.greengrowthknowledge.org/sites/default/files/downloads/resource/Sustainable_Infrastructure_and_Finance_UNEPInquiry.pdf.
- Federal Statistical Office of Germany (Destatis). 2020. *Death Statistics*. Destatis. https://www.destatis.de/EN/Themes/Society-Environment/Population/Deaths-Life-Expectancy/_node.html.
- Federal Statistical Office of Germany (Destatis). 2020. *Medical facilities, hospital beds and movement of patient 2020*. Destatis. <https://www.destatis.de/EN/Themes/Society-Environment/Health/Hospitals/Tables/gd-hospitals-laender.html>.
- Founda, D., & Santamouris, M. (2017). Synergies between Urban Heat Island and Heat Waves in Athens (Greece), during an extremely hot summer (2012). *Scientific reports*, 7(1), 1-11. <https://doi.org/10.1038/s41598-017-11407-6>.
- García-Cueto, O. R., López-Velázquez, J. E., Bojórquez-Morales, G., Santillán-Soto, N. & Flores-Jiménez, D. E. (2021). Trends in temperature extremes in selected growing cities of Mexico under a non-stationary climate. *Atmósfera*, 34(3), 233–254. <https://doi.org/10.20937/ATM.52784>.
- Ghada, W., Estrella, N., Ankerst, D. P., & Menzel, A. (2021). Universal thermal climate index associations with mortality, hospital admissions, and road accidents in Bavaria. *PLoS one*, 16(11), e0259086. <https://doi.org/10.1371/journal.pone.0259086>.
- Great Britain. Health, & Safety Commission. (1988). *Comments Received on the Tolerability Risk from Nuclear Power Stations*. HM Stationery Office.
- Great Britain. Health, & Safety Commission. (1991). *Major hazard aspects of the transport of dangerous substances*. Report and appendices. London: Advisory Committee on Dangerous Substances.
- Green Factor Measurement, City of Seattle Municipal Code §23.86.019 (2021). https://library.municode.com/wa/seattle/codes/municipal_code?nodeId=13857.
- Hansen, S.O., Höffer, R., Rees, J., Ricciardelli, F., Spehl, P. (2019). Towards the Second Generation Eurocodes: Evolution of EN 1991-1-4 Wind Actions. In: Ricciardelli, F., Avossa, A. (eds) Proceedings of the XV Conference of the Italian Association for Wind

- Engineering. IN VENTO 2018. Lecture Notes in Civil Engineering, vol 27. Springer, Cham. https://doi.org/10.1007/978-3-030-12815-9_28.
- Heaviside, C., Macintyre, H. & Vardoulakis, S. (2017) The Urban Heat Island: Implications for Health in a Changing Environment. *Curr Envir Health Rpt* 4, 296–305. <https://doi.org/10.1007/s40572-017-0150-3>.
- Heris, M. P., Middel, A., & Muller, B. (2020). Impacts of form and design policies on urban microclimate: Assessment of zoning and design guideline choices in urban redevelopment projects. *Landscape and Urban Planning*, 202, 103870. <https://doi.org/10.1016/j.landurbplan.2020.103870>.
- Hibbard, K.A., Hoffman, F.M., Huntzinger, D. & West, T.O. (2017). Changes in land cover and terrestrial biogeochemistry. In *Climate Science Special Report: Fourth National Climate Assessment, Volume I* [Wuebbles, D.J., D.W. Fahey, K.A. Hibbard, D.J. Dokken, B.C. Stewart, and T.K. Maycock (eds.)]. U.S. Global Change Research Program, Washington, DC. pp. 277–302. <https://science2017.globalchange.gov/chapter/10/>.
- Ibrahim, Y., Kershaw, T., Shepherd, P., & Coley, D. (2021). On the Optimization of Urban form Design, Energy Consumption and Outdoor Thermal Comfort Using a Parametric Workflow in a Hot Arid Zone. *Energies* 2021, 14 (4026). <https://doi.org/10.3390/en14134026>.
- International Organization for Standardization (2015). *ISO 2394:2015 - General Principles on Reliability for Structures*. Geneva.
- IPCC, 2021: *Climate Change 2021: The Physical Science Basis. Contribution of Working Group I to the Sixth Assessment Report of the Intergovernmental Panel on Climate Change* [Masson-Delmotte, V., P. Zhai, A. Pirani, S.L. Connors, C. Péan, S. Berger, N. Caud, Y. Chen, L. Goldfarb, M.I. Gomis, M. Huang, K. Leitzell, E. Lonnoy, J.B.R. Matthews, T.K. Maycock, T. Waterfield, O. Yelekçi, R. Yu, and B. Zhou (eds.)]. Cambridge University Press. In Press. <https://www.ipcc.ch/report/ar6/wg1/#FullReport>.
- Jacob, D., Petersen, J., Eggert, B., Alias, A., Christensen, O. B., Bouwer, L. M., ... & Yiou, P. (2014). EURO-CORDEX: new high-resolution climate change projections for European impact research. *Regional environmental change*, 14(2), 563-578. <https://doi.org/10.1007/s10113-013-0499-2>.
- Kamal, A., Abidi, S. M. H., Mahfouz, A., Kadam, S., Rahman, A., Hassan, I. G., & Wang, L. L. (2021). Impact of urban morphology on urban microclimate and building energy loads. *Energy and Buildings*, 253, 111499. <https://doi.org/10.1016/j.enbuild.2021.111499>.
- Kasperski, Michael. (2002). A new wind zone map of Germany. *Journal of Wind Engineering and Industrial Aerodynamics*, 90. 1271-1287. [https://doi.org/10.1016/S0167-6105\(02\)00257-X](https://doi.org/10.1016/S0167-6105(02)00257-X).
- Liel, A. B., & Deierlein, G. G. (2012). Using collapse risk assessments to inform seismic safety

- policy for older concrete buildings. *Earthquake spectra*, 28(4), 1495-1521.
<https://doi.org/10.1193/1.4000090>.
- Lombardo, F. T., Main, J. A., & Simiu, E. (2009). Automated extraction and classification of thunderstorm and non-thunderstorm wind data for extreme-value analysis. *Journal of Wind Engineering and Industrial Aerodynamics*, 97(3-4), 120-131.
<https://doi.org/10.1016/j.jweia.2009.03.001>.
- Marx, W., Haunschild, R., & Bornmann, L. (2021). Heat waves: a hot topic in climate change research. *Theoretical and Applied Climatology*, 146(1), 781-800.
<https://doi.org/10.1007/s00704-021-03758-y>.
- Meynen, E., & Schmithüsen, J., Gellert, J., Neef, E., Müller-Miny, H., & Schultze, J.H. (1962). *Handbuch der naturräumlichen Gliederung Deutschlands [Handbook of the natural spatial structure of Germany]*. Bad Godesberg.
- Muthers, S., Laschewski, G., & Matzarakis, A. (2017). The Summers 2003 and 2015 in South-West Germany: Heat Waves and Heat-Related Mortality in the Context of Climate Change. *Atmosphere*, 8(11), 224. <https://doi.org/10.3390/atmos8110224>.
- Nakano, A., Bueno, B., Norford, L., & Reinhart, C. F. (2015) Urban Weather Generator - a Novel Workflow for Integrating Urban Heat Island Effect within Urban Design Process. *Proceedings of the 14th Conference of International Building Performance Simulation Association BS2015, 7-9 December, 2015, Hyderabad, India*.
- The Netherlands Ministry of Housing, Spatial Planning and the Environment (VROM). (2004). *Besluit Externe Veiligheid Inrichtingen [External Safety (Establishments) Decree]*. Staatsblad.
- NOAA National Centers for Environmental Information. (2021). *Global Surface Hourly, Kempten Durach, GM*. <https://www.ncei.noaa.gov/metadatas/geoportals/rest/metadatas/item/gov.noaa.ncdc%3AC00532/html>.
- NOAA. (2020). *Weather related fatality and injury statistics*. National Weather Service.
<https://www.weather.gov/hazstat/>.
- Orru, H., Åström, C., Andersson, C., Tamm, T., Ebi, K. L., & Forsberg, B. (2019). Ozone and heat-related mortality in Europe in 2050 significantly affected by changes in climate, population and greenhouse gas emission. *Environmental Research Letters*, 14(7), 074013. <https://doi.org/10.1088/1748-9326/ab1cd9>.
- Planning and Zoning, Code of the City of Portland, Oregon §33.510 (2020).
<https://www.portland.gov/code/33>.
- Planning Department, Hong Kong Government. (1993). *Hong Kong Planning Standards and Guidelines*. Hong Kong: Government Printer.
- Planning, NSW. (1992). Risk criteria for land use safety planning. Hazardous Industry Planning advisory Paper No 4. *Planning NSW is now Department of Infrastructure, Planning and Natural Resources, DIPNR*.

- O'Rourke, M., Koch, P., and Redfield, R. (1983). Analysis of roof snow load case studies: Uniform loads." U.S. Department of the Army, Cold Regions Research and Engineering Laboratory, Hanover, N.H., CRREL Report No. 83-1.
- Oke, T.R. (1987). *Boundary Layer Climates*. London: Methuen and Company, Print.
- Peterka, J. A. (1992). "Improved extreme wind prediction for the United States." *J. Wind Engrg. Industrial Aerodynamics*, 41, 533–541.
- Peterka, J. A., and Shahid, S. (1993). "Extreme gust wind speeds in the U.S." In *Proceedings of the 7th U.S. National Conference on Wind Engineering*, Gary Hart, ed., 2, 503–512.
- Peterka, J. A., and Shahid, S. (1998). "Design gust wind speeds in the United States." *J. Struct. Engrg.*, 124(2), 207–214.
- Rahman, M. A., Moser, A., Rötzer, T., & Pauleit, S. (2017). Within canopy temperature differences and cooling ability of *Tilia cordata* trees grown in urban conditions. *Building and Environment*, 114, 118-128. <https://doi.org/10.1016/j.buildenv.2016.12.013>.
- Rhomberg, L. R. (1997). A survey of methods for chemical health risk assessment among Federal regulatory agencies. *Human and Ecological Risk Assessment: An International Journal*, 3(6), 1029-1196. <https://doi.org/10.1080/10807039709383746>.
- Richard, Y., Pohl, B., Rega, M., Pergaud, J., Thevenin, T., Emery, J., ... & Chateau-Smith, C. (2021). Is Urban Heat Island intensity higher during hot spells and heat waves (Dijon, France, 2014–2019)? *Urban Climate*, 35, 100747. <https://doi.org/10.1016/j.uclim.2020.100747>.
- Rohat, G., Flacke, J., Dosio, A., Pedde, S., Dao, H., & van Maarseveen, M. (2019). Influence of changes in socioeconomic and climatic conditions on future heat-related health challenges in Europe. *Global and planetary change*, 172, 45-59. <https://doi.org/10.1016/j.gloplacha.2018.09.013>.
- Roudsari, M. S., Pak, M., & Smith, A. (2013). Ladybug: a parametric environmental plugin for grasshopper to help designers create an environmentally-conscious design. In *Proceedings of the 13th international IBPSA conference held in Lyon, France Aug* (pp. 3128-3135). http://www.ibpsa.org/proceedings/BS2013/p_2499.pdf.
- Russo, S., Sillmann, J., & Fischer, E. M. (2015). Top ten European heatwaves since 1950 and their occurrence in the coming decades. *Environmental Research Letters*, 10(12), 124003. <https://doi.org/10.1088/1748-9326/10/12/124003>.
- Sailor, D., Shepherd, M., Sheridan, S., Stone, B., Kalkstein, L., Russell, A., ... & Andersen, T. (2016). Improving heat-related health outcomes in an urban environment with science-based policy. *Sustainability*, 8(10), 1015. <https://doi.org/10.3390/su8101015>.
- Salvati, A., Palme, M., & Inostroza, L. (2017). Key parameters for urban heat island assessment in a Mediterranean context: A sensitivity analysis using the Urban Weather Generator model. In *IOP Conference Series: Materials Science and Engineering* (Vol.

- 245, No. 8, p. 082055). IOP Publishing. <https://doi.org/10.1088/1757-899X/245/8/082055>.
- Sanpaolesi, L., Del Corso, R., Formichi, P., Currie, D., Sims, P., Sacré, C., Stiefel, U., Lozza, S., Eiselt, B., Peckham, R., et al. (1998). *Phase 1 Final Report to the European Commission, Scientific Support Activity in the Field of Structural Stability of Civil Engineering Works: Snow Loads*; Department of Structural Engineering, University of Pisa: Pisa, Italy, 1998. http://www2.ing.unipi.it/dic/snowloads/Final_Report_I.pdf.
- Spouge, J., Skjong, R., & Olufsen, O. (2015). Risk Acceptance and Cost Benefit Criteria Applied in the Maritime Industry in Comparison with Other Transport Modes and Industries. In *Proceedings of the 12th International Conference on the Stability of Ships and Ocean Vehicles, Glasgow, Scotland*, p. 283–292.
- Strandberg, G., Barring, L., Hansson, U., Jansson, C., Jones, C., Kjellström, E., Kolax, M., Kupiainen, M., Nikulin, G., Samuelsson, P., Ullerstig, A. & Wang, S. (2014). CORDEX scenarios for Europe from the Rossby Centre regional climate model RCA4. SMHI Report: Meteorology and Climatology No. 116, 2014. <http://smhi.diva-portal.org/smash/get/diva2:948136/FULLTEXT01.pdf>.
- Supian, N. M. & Hasan, H. (2021). *Selecting the probability distribution of annual maximum temperature in Malaysia*. ITM Web of Conferences. <https://doi.org/10.1051/itmconf/20213601010>.
- Tanarhte, M., Hadjinicolaou, P. & Lelieveld, J. (2015). Heat wave characteristics in the eastern Mediterranean and Middle East using extreme value theory. *Climate Research*, 63, 99–113. <https://doi.org/10.3354/cr01285>.
- Tanner, P., & Hingorani, R. (2015). Acceptable risks to persons associated with building structures. *Structural Concrete*, 16(3), 314-322. <https://doi.org/10.1002/suco.201500012>.
- Tree Shading Requirements for Parking Lots, Sacramento City Code §17.612.040 (2021). <http://www.qcode.us/codes/sacramento/?view=desktop&topic=0>.
- Tsang, HH., Daniell, J.E., Wenzel, F., & Wilson, J. (2020). A universal approach for evaluating earthquake safety level based on societal fatality risk. *Bull Earthquake Eng* 18, 273–296. <https://doi.org/10.1007/s10518-019-00727-9>.
- Twumasi-Ankrah, S. & Nyantakyi, A. (2019). Statistical Modeling of Temperature Extremes Behaviour in Ghana. *Journal of Mathematics and Statistics*, 14(1), 275-284. <https://doi.org/10.3844/jmssp.2018.275.284>.
- United Nations, Department of Economic and Social Affairs, Population Division. (2019). *World Urbanization Prospects: The 2018 Revision (ST/ESA/SER.A/420)*. New York: United Nations.
- U.S. Department of Energy (DOE), (1991). *Department of Energy Nuclear Safety Policy*. U.S. Department of Energy, Washington, DC.
- U.S. Nuclear Regulatory Commission (NRC). (1995). *Use of Probabilistic Risk Assessment*

Methods in Nuclear Regulatory Activities; Final Policy Statement. U.S. Nuclear Regulatory Commission, Washington, DC.

U.S. Nuclear Regulatory Commission (NRC). (2011). *Technical basis for regulatory guidance on design-basis hurricane wind speeds for nuclear power plants* (NUREG/CR-7005).

U.S. Nuclear Regulatory Commission, Washington, DC.

Wu, Z. and Ren, Y. (2018). A bibliometric review of past trends and future prospects in urban heat island research from 1990 to 2017. *Environmental Reviews*. 27(2): 241-251.

<https://doi.org/10.1139/er-2018-0029>.

Yiou, P., Cattiaux, J., Faranda, D., Kadyrov, N., Jézéquel, A., Naveau, P., Ribes, A., Robin, Y., Thao, S., Van Oldenborgh, G. & Vrac, M. (2020). Analyses of the Northern European summer heatwave of 2018. *Bulletin of the American Meteorological Society*, 101(1), S35-S40.

<https://doi.org/10.1175/BAMS-D-19-0170.1>.

Zhao, L., Oppenheimer, M., Zhu, Q., Baldwin, J. W., Ebi, K. L., Bou-Zeid, E., ... & Liu, X.

(2018). Interactions between urban heat islands and heat waves. *Environmental research letters*, 13(3), 034003. <https://doi.org/10.1088/1748-9326/aa9f73>.

List of Figures

Figure 1-1: Typical distribution of temperatures in UHI (Figure 8.12 from Oke, 1987)	8
Figure 2-1: Trend of publications on heatwaves (Fig.1 from Marx, Haunschild and Bormmann, 2021)	11
Figure 2-2: Co-occurrence network map of publications on heatwaves (Fig. 4 from Marx, Haunschild and Bornmann, 2021).	12
Figure 2-3: Proposal for new wind load maps for Germany (Fig. 10. from Kasperski, 2002)	15
Figure 2-4: FN curves of the upper bound of ALARP region from various standards and guidelines (Fig. 7 from Tsang et al., 2020)	17
Figure 3-1: Map of study area: Kempten, Germany	19
Figure 3-2: Satellite image of study area (Google Maps)	19
Figure 3-3: Location of weather stations by governmental districts	23
Figure 3-4: Excess heat-mortality exposure-response curve for Bavaria (Fig. 1 from Breitner et al., 2014)	24
Figure 3-5: Risk-based framework for developing UHI design criteria	26
Figure 4-1: Population adjusted FN curve for southern Germany ($\lambda_{D,tolerable} = 10^{-6}$, $N_{R,max} = 0.0003P$ & $b=2.0$)	30
Figure 4-2: Exceedance probability curves with 95% confidence intervals of tas (top) & UHI_{tot} of the study area (bottom)	33
Figure 4-3: Exceedance probability curves of tas & UHI_{tot} of the study area	33
Figure 5-1: Plot of reference residential districts and their urban density parameters	36
Figure A-1: UHI diurnal pattern for hottest week in 1991	52

List of Tables

Table 3-1: Description of input parameters for UHI modelling	28
Table 4-1: $N_{tolerable}$ based on a range of risk parameters.....	31
Table 4-2: $UHII_{design}$ in Celsius based on a range of risk parameters	32
Table 4-3: $UHII_{50}$ in Celsius based on different scenarios of tree cover, footprint density, and façade-to-site ratio;.....	34
Table A-1: Comparison of top ten hottest weeks (in °C) from different datasets	51
Table A-2: tas , UHI , and $UHII$ for Kempten by year	51
Table C-1: GCM-RCM combinations of publicly available EURO-CORDEX output for tas_{max} at 0.11° spatial resolution	61

Appendix

A.1. Weather Data

Table A-1: Comparison of top ten hottest weeks (in °C) from different datasets

(a) Kempton (NOAA)			(b) Kempton (DWD)			(c) Southern Germany (DWD)		
<i>tas</i>	Year	Dates	<i>tas</i>	Year	Dates	<i>tas</i>	Year	Dates
23.31°	1983	25.07-31.07	23.99°	2015	01.07-07.07	27.25°	2003	04.08-10.08
21.31°	1991	06.07-12.07	23.74°	2019	25.06-01.07	26.39°	1957	02.07-08.07
20.81°	1982	10.07-16.07	23.31°	1983	25.07-31.07	26.02°	2015	01.07-07.07
20.66°	1992	03.08-09.08	23.27°	2003	04.08-10.08	25.90°	2018	30.07-05.08
20.64°	1976	30.06-06.07	23.13°	1952	01.07-07.07	25.60°	1983	25.07-31.07
20.57°	1986	29.07-04.08	23.11°	2018	31.07-06.08	25.42°	2006	20.07-26.07
20.53°	1984	08.07-14.07	22.99°	2002	17.06-23.06	25.11°	1976	28.06-04.07
20.46°	1981	31.07-06.08	22.81°	2006	20.07-26.07	25.06°	2019	25.07-31.07
20.20°	1980	01.08-07.08	22.69°	1957	02.07-08.07	25.01°	1964	15.07-21.07
20.14°	1987	29.06-05.07	22.69°	2010	08.07-14.07	24.62°	1994	31.07-06.08

Table A-2: *tas*, *UHI*, and *UHII* for Kempton by year

<i>tas</i> (°C)	<i>UHI</i> (°C)	<i>UHII</i> (°C)	Year
18.68°	18.88°	0.19°	1973
20.34°	20.52°	0.17°	1974
19.13°	19.32°	0.18°	1975
20.59°	20.83°	0.23°	1976
18.54°	18.74°	0.19°	1977
20.03°	20.18°	0.14°	1978
19.07°	19.23°	0.15°	1979
20.91°	21.05°	0.13°	1980
20.61°	20.74°	0.13°	1981
21.40°	21.55°	0.15°	1982
24.05°	24.22°	0.17°	1983
20.67°	20.84°	0.16°	1984
20.91°	21.04°	0.13°	1985
20.91°	21.08°	0.17°	1986
20.38°	20.56°	0.18°	1987
20.04°	20.19°	0.15°	1988
19.57°	19.71°	0.13°	1989
20.96°	21.15°	0.19°	1991
21.37°	21.52°	0.14°	1992

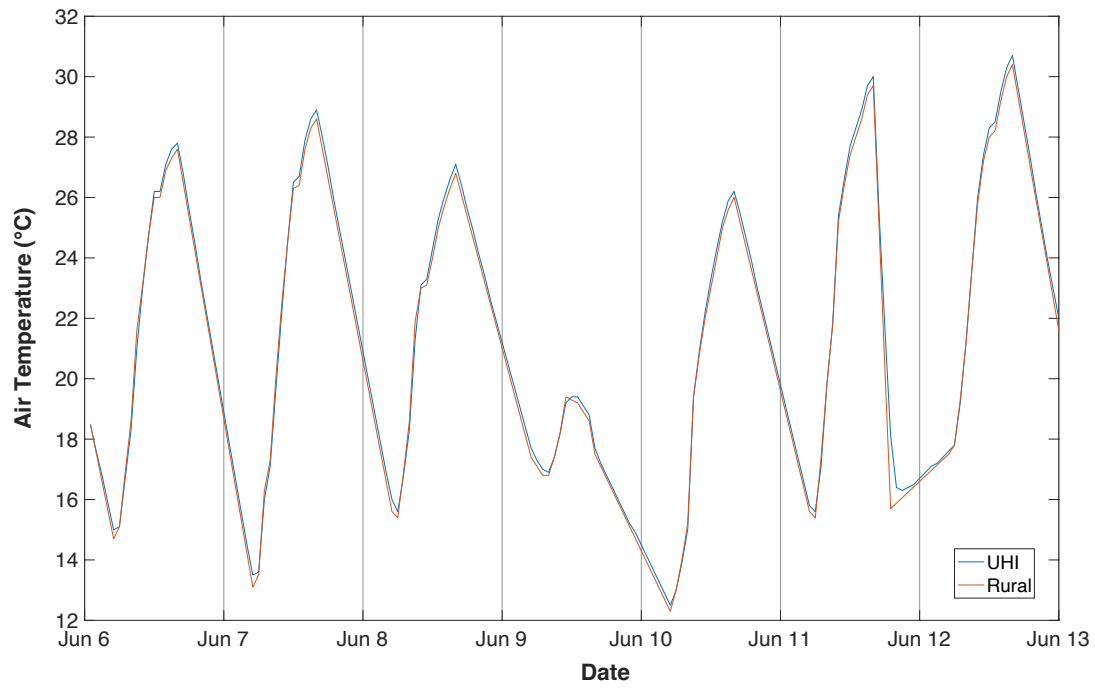


Figure A-1: UHI diurnal pattern for hottest week in 1991

B.1. Sample MATLAB Script

Contents

- import annual hottest week avg temp of Kempton (1973-1989, 1991-1992)
- MLE of the parameters and CI95 parameters for GEV distribution of the weather data. Parmhat(1) is the shape parameter, k, parmhat(2) is the scale parameter, sigma, and parmhat(3) is the location parameter, mu
- histogram of historical data plotted against GEV pdf with mle parameters
- Plot theoretical and empirical MRI curve
- Calculation of 50-yr extreme heat (minor interpolation used)
- Plot theoretical MRI curve for CI95 upper
- Calculation of 50-yr extreme heat for CI95 lower (minor interpolation used)
- Plot theoretical MRI curve for CI95 Lower
- Calculation of 50-yr extreme heat for CI95 lower (minor interpolation used)
- Calculation of UHII w/ CI95

```
clc, clear, close all
```

import annual hottest week avg temp of Kempton (1973-1989, 1991-1992)

```
DaysPerYear = 122;

% Rural daily mean converted to annual hottest (NOAA)
weekly_rollingavgtemp_Kempton = readmatrix('tas_06_09_1973_1992.xlsx','range','B3:B2320');

TotalYears = floor(length(weekly_rollingavgtemp_Kempton)/DaysPerYear);

annual_maxtemp_Kempton = zeros(TotalYears,1);

for yearindex = 0:TotalYears-1
    for dayindex = 1:DaysPerYear
        if annual_maxtemp_Kempton(yearindex+1) < weekly_rollingavgtemp_Kempton(dayindex+DaysPerYear*yearindex)
            annual_maxtemp_Kempton(yearindex+1) = weekly_rollingavgtemp_Kempton(dayindex+DaysPerYear*yearindex);
        end
    end
end

% UHI annual hottest week w/o new development (from UWG)
UHI_annual_maxtemp_Kempton = readmatrix('UHIMaxWeeklyAvgTempKempton73_92.xlsx','range','A1:A19');

% UHI daily mean converted to annual hottest week w/ new development (from UWG)
weekly_rollingavgtempUHI_NB_Kempton = readmatrix('MinTreeMinBuildingDailyAvgTempUHINewBuildings1973-1992.xlsx','range','B3:B2320');

TotalYears = floor(length(weekly_rollingavgtempUHI_NB_Kempton)/DaysPerYear);
UHI_NB_annual_maxtemp_Kempton = zeros(TotalYears,1);

for yearindex = 0:TotalYears-1
    for dayindex = 1:DaysPerYear
        if UHI_NB_annual_maxtemp_Kempton(yearindex+1) < weekly_rollingavgtempUHI_NB_Kempton(dayindex+DaysPerYear*yearindex)
            UHI_NB_annual_maxtemp_Kempton(yearindex+1) = weekly_rollingavgtempUHI_NB_Kempton(dayindex+DaysPerYear*yearindex);
        end
    end
end
```

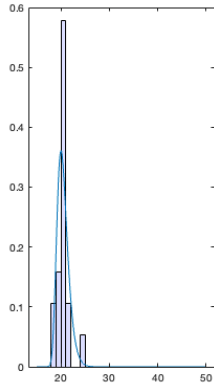
MLE of the parameters and CI95 parameters for GEV distribution of the weather data. Parmhat(1) is the shape parameter, k, parmhat(2) is the scale parameter, sigma, and parmhat(3) is the location parameter, mu

```
[paramEsts,paramCI] = gevfit(annual_maxtemp_Kempton);
[UHI_paramEsts,UHI_paramCI] = gevfit(UHI_annual_maxtemp_Kempton);
[UHI_NB_paramEsts,UHI_NB_paramCI] = gevfit(UHI_NB_annual_maxtemp_Kempton);
```

histogram of historical data plotted against GEV pdf with mle parameters

```
figure(1)
tiledlayout(1,2)
nexttile

histogram(annual_maxtemp_Kempton,15:50,'FaceColor',[.8 .8 1],'Normalization','probability');
xgrid = linspace(15,50,1000);
line(xgrid,gevpdf(xgrid,paramEsts(1),paramEsts(2),paramEsts(3)));
```



Plot theoretical and empirical MRI curve

```

% Empirical CDF
[p,x]=ecdf(annual_maxtemp_Kempton);
E_MRI_annual_maxtemp_Kempton = 1 ./ (1 - p);

[UHI_p,UHI_x]=ecdf(UHI_annual_maxtemp_Kempton);
UHI_E_MRI_annual_maxtemp_Kempton = 1 ./ (1 - UHI_p);

[UHI_NB_p,UHI_NB_x]=ecdf(UHI_NB_annual_maxtemp_Kempton);
UHI_NB_E_MRI_annual_maxtemp_Kempton = 1 ./ (1 - UHI_NB_p);

% Exceedence Probability & MRI of theoretical temps
y = 1 - gevpdf(xgrid, paramEsts(1), paramEsts(2), paramEsts(3));
logy = 1./y;

UHI_y = 1 - gevpdf(xgrid, UHI_paramEsts(1), UHI_paramEsts(2), UHI_paramEsts(3));
UHI_logy = 1./UHI_y;

UHI_NB_y = 1 - gevpdf(xgrid, UHI_NB_paramEsts(1), UHI_NB_paramEsts(2), UHI_NB_paramEsts(3));
UHI_NB_logy = 1./UHI_NB_y;

% Finds index of MRI 1 to 1000
[thousandyr,i_thousandyr] = min(abs(logy - 1000));
for i = 1:length(xgrid)
    mri = logy(i);
    if mri > 1
        i_oneyr = i;
        break
    end
end

[UHI_thousandyr,UHI_i_thousandyr] = min(abs(UHI_logy - 1000));
for j = 1:length(xgrid)
    UHI_mri = UHI_logy(j);
    if UHI_mri > 1
        UHI_i_oneyr = j;
        break
    end
end

[UHI_NB_thousandyr,UHI_NB_i_thousandyr] = min(abs(UHI_NB_logy - 1000));
for m = 1:length(xgrid)
    UHI_NB_mri = UHI_NB_logy(m);
    if UHI_NB_mri > 1
        UHI_NB_i_oneyr = m;
        break
    end
end

% Theoretical temps and MRI
trunc_logy = logy(i_oneyr:i_thousandyr);
theoretical_temps = xgrid(i_oneyr:i_thousandyr);

UHI_trunc_logy = UHI_logy(UHI_i_oneyr:UHI_i_thousandyr);
UHI_theoretical_temps = xgrid(UHI_i_oneyr:UHI_i_thousandyr);

UHI_NB_trunc_logy = UHI_NB_logy(UHI_NB_i_oneyr:UHI_NB_i_thousandyr);
UHI_NB_theoretical_temps = xgrid(UHI_NB_i_oneyr:UHI_NB_i_thousandyr);

% Plot theoretical and empirical MRI curve

```



```

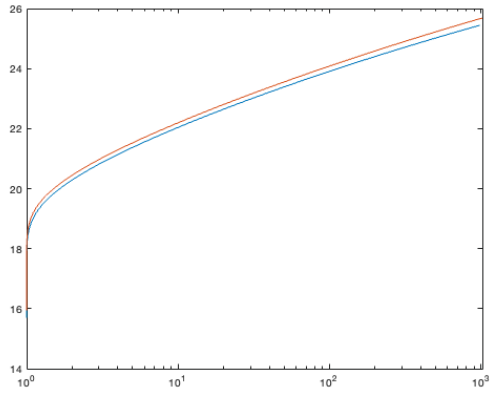
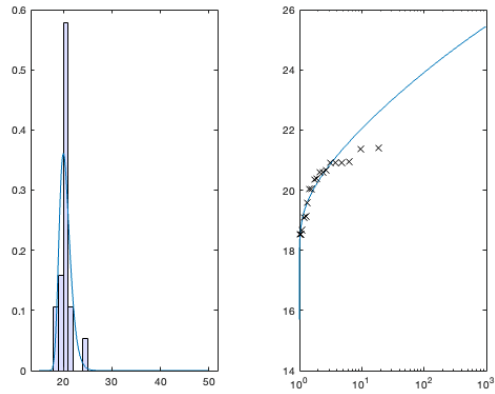
nexttile
semilogx(trunc_logy,theoretical_temps)
hold on
semilogx(E_MRI_annual_maxtemp_Kempton,x,'x','Color',[0 0 0]);

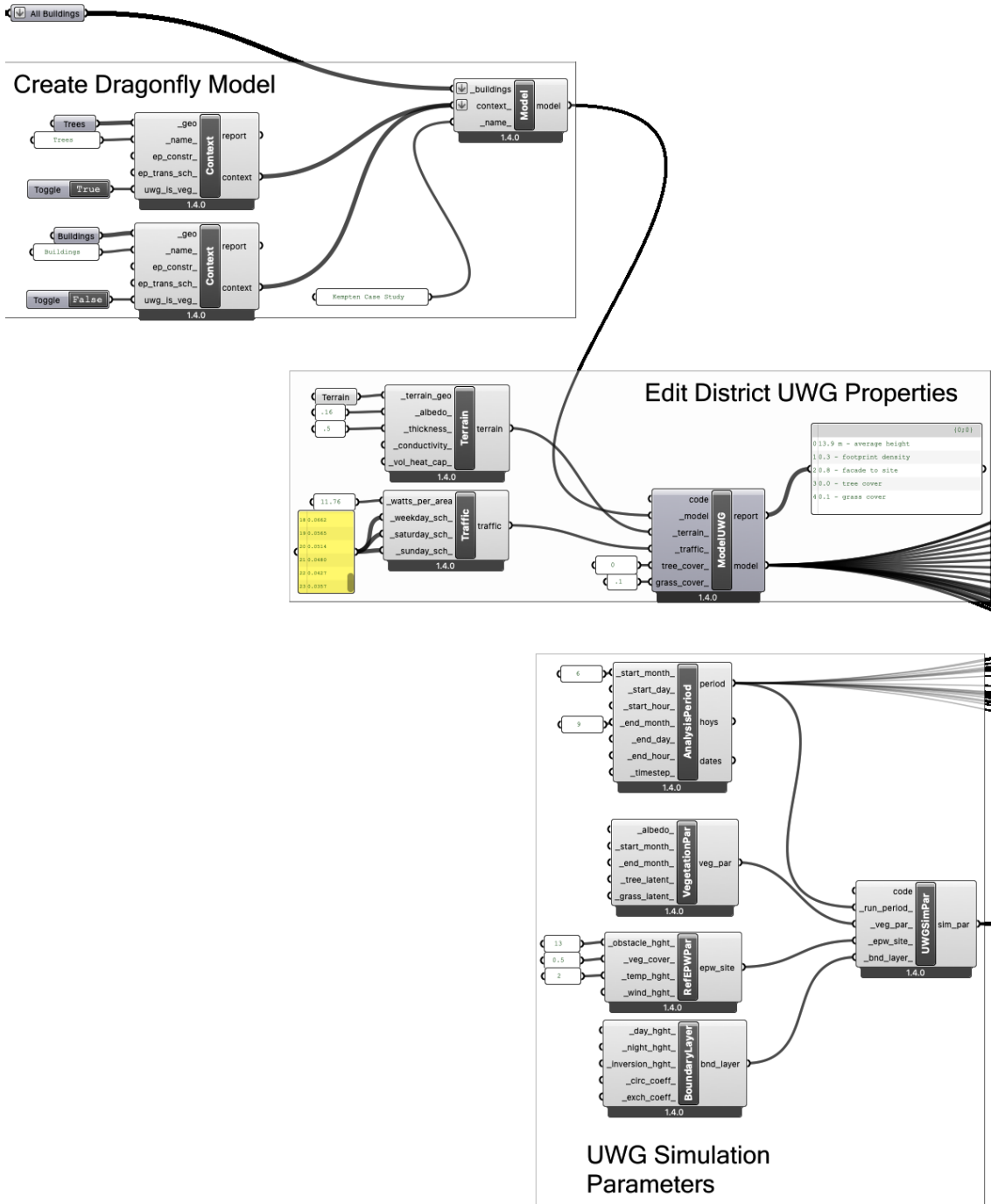
figure(2)
semilogx(trunc_logy,theoretical_temps)
hold on
semilogx(UHI_NB_trunc_logy,UHI_NB_theoretical_temps)
hold off

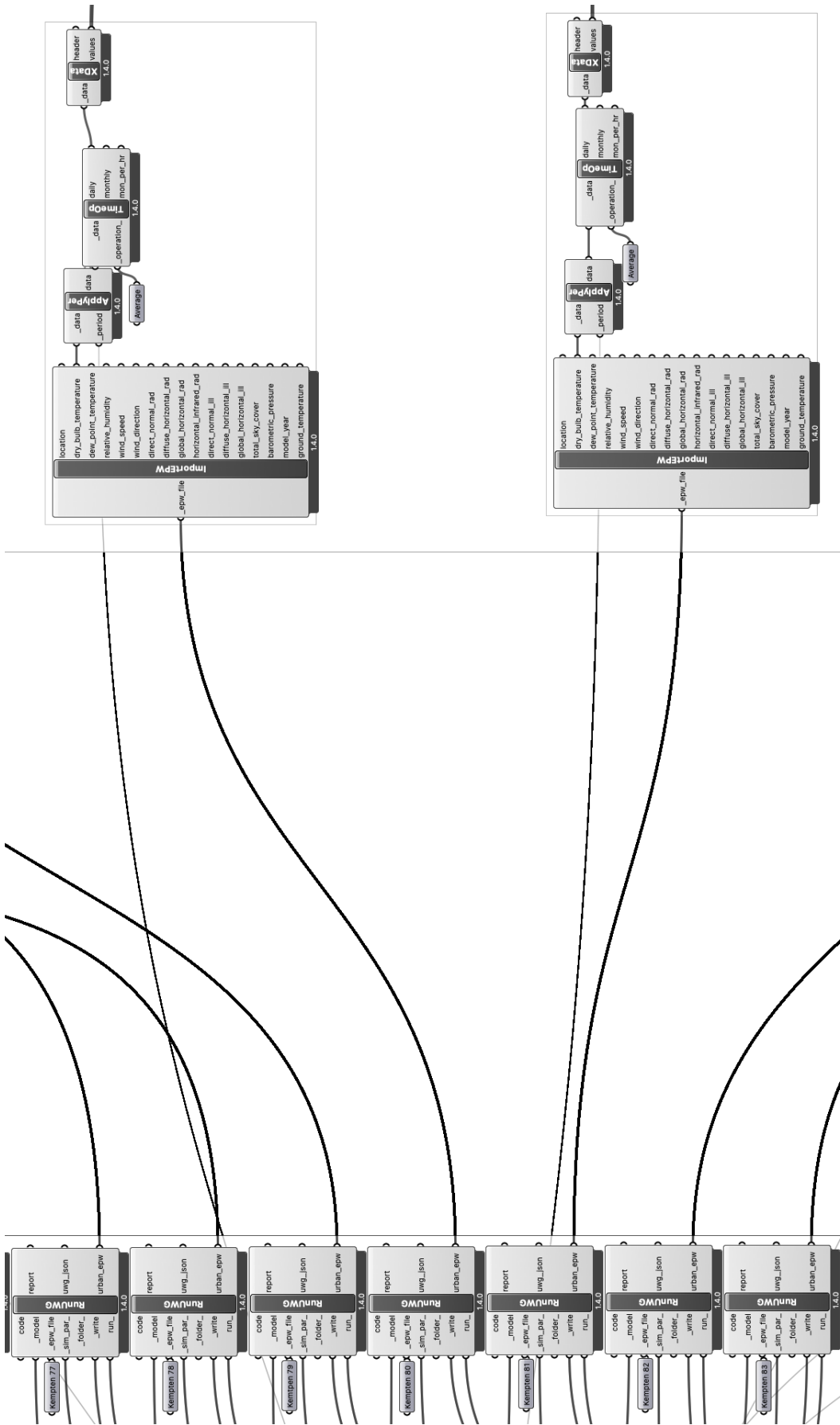
figure(3)
t = tiledlayout(2,1);
nexttile(1)
semilogx(trunc_logy,theoretical_temps)
hold on

figure(3)
nexttile(2)
semilogx(UHI_NB_trunc_logy,UHI_NB_theoretical_temps)
hold on

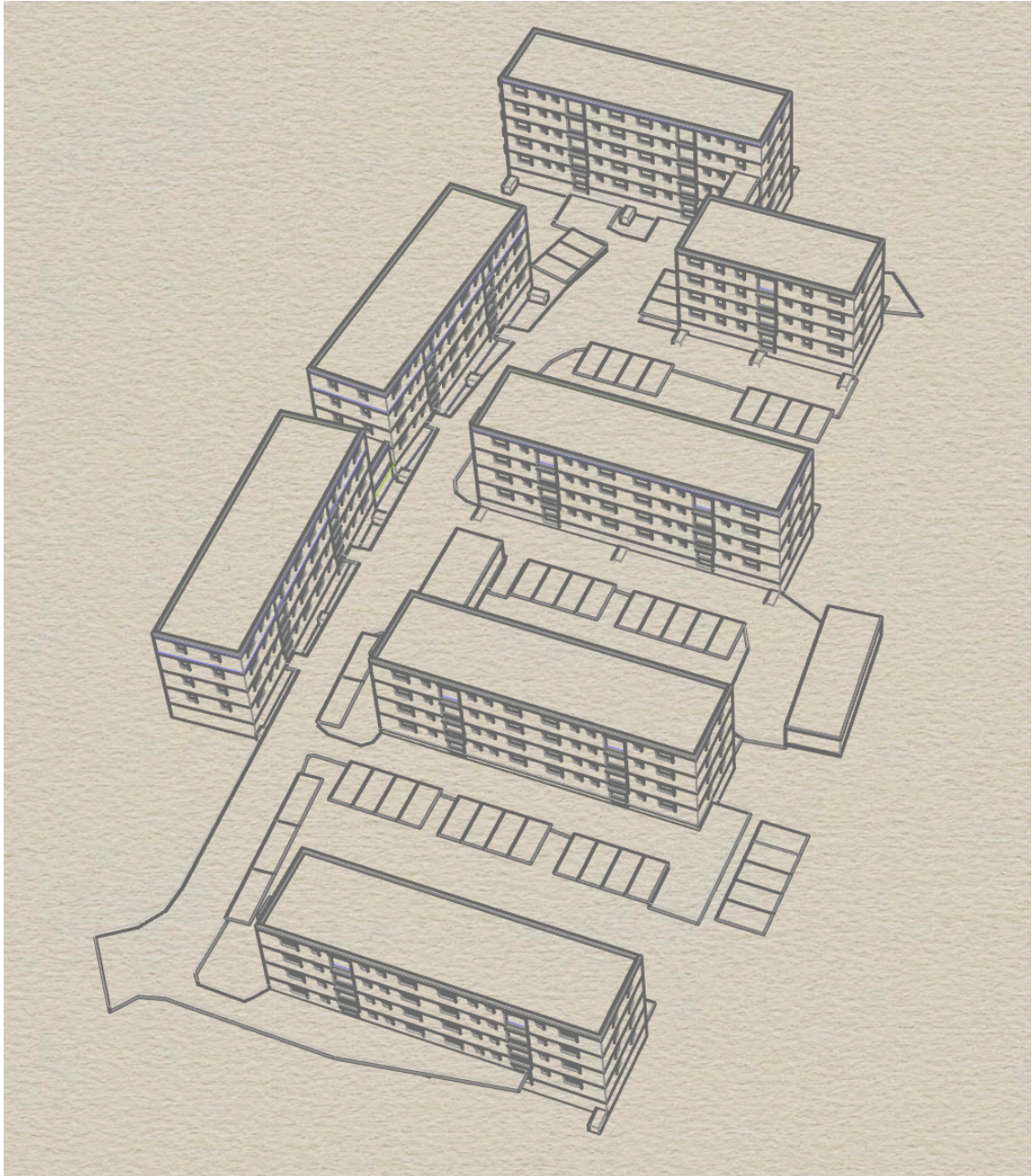
```







B.3. Building Model of Study Area



C.1. Climate Models for Future Scenarios

The choice of climate models to provide data for projecting extreme heat is not trivial. Climate modelling is a complex field with relatively large uncertainties. The challenge of minimizing uncertainties lies in the modelling itself, but the understanding of the behavior of climate models is equally important when it comes to projecting extreme heat.

For localized extreme heat projections, climate data from the EURO-CORDEX is a good candidate due to the reliability, availability and resolution of its data. The EURO-CORDEX is a coordinated set of downscaling experiments (European component of CORDEX) that includes climate models from a lot of the major climate institutes in Europe (Jacob et al., 2014). This coordination ensures that the experiment protocols, forcings and output are all consistent. Within the EURO-CORDEX, GCMs from CMIP5 are downscaled to RCMs. CMIP5 are a set of coordinated GCM experiments and was the main climate modeling resource used by the IPCC for AR5. CMIP6 used by the IPCC for AR6, which contains newer experiments than CMIP5 was not used because experiments are still being downscaled and as a result, much regional climate data is still not available. GCMs by themselves provide output with spatial resolutions of approximately 1000 km by 1000 km. This is insufficient for assessing extreme heat at the localized level. On the other hand, RCMs in the EURO-CORDEX provide output with a 12.5 km by 12.5 km spatial resolution. The organization of available RCMs and GCMs combinations for 12.5 km by 12.5 km for tas_{max} is depicted in Table C-1. The only RCMs with data available for all three RCP scenarios are RCA4, HIRHAM5 and ALADIN63. The climate data is available on the ESGF online database.

Within the regional downscaling process, RCMs are driven by a particular GCM. There are a lot of factors at this stage that affect temperature projections, which make the choice of RCM-GCM combinations non-trivial. One example is the lack of time-varying anthropogenic aerosols used for most of the RCMs except for ALADIN53 and ALADIN63 (Boé et al., 2020). Boé et al. (2020) has pointed out that this causes the RCMs to project lower temperatures than the GCMs that drive them. This is due to the fact that global dimming is reduced if the trend of decreasing anthropogenic aerosols is accounted for. In other words, the RCMs other than ALADIN53 and ALADIN63 estimate future climate with greater amounts of anthropogenic aerosols which as a result projects lower temperatures. Strandberg et al. (2014) has also observed a cold bias for

the RCM RCA4. RCA4 was found to give smaller temperature increases than the GCMs in the summer for most of Europe including for west central Europe (Strandberg et al., 2014). Based on these considerations of the available models (Table C-1), the ALADIN63 – CNRM-CM5 was the most appropriate for this paper.

Regional Climate Models	Driving Global Coupled Models							
	HadGEM2-ES (MOHC)	EC-EARTH (IHEC)	CNRM-CM5 (CNRM-CERFACS)	NorESM1-M (NCC)	MPI-ESM-LR (MPI)	IPSL-CM5A-MIR (IPSL)	MIROC5 (MIROC)	
RCA4 (SMHI)	RCP2.6	RCP2.6	RCP2.6	RCP2.6	RCP2.6	RCP2.6	RCP2.6	
CCLM4-8-17 (CLMcom)								RCP8.5
HIRHAM5 (DMI)	RCP2.6	RCP2.6	RCP2.6	RCP2.6	RCP2.6	RCP2.6	RCP2.6	
WRF361H (UHOH)								
WRF381P (IPSL)		RCP2.6			RCP2.6		RCP2.6	
ALADIN53 (CNRM)			RCP2.6					
ALADIN63 (CNRM)		RCP2.6	RCP2.6		RCP2.6		RCP2.6	
RegCM4-6 (ICTP)								
HadREM3-GA7-05 (MOHC)	RCP2.6	RCP2.6	RCP2.6		RCP2.6		RCP2.6	

N/A	RCP2.6	RCP4.5	RCP8.5
-----	--------	--------	--------

Table C-1: GCM-RCM combinations of publicly available EURO-CORDEX output for tas_{max} at 0.11° spatial resolution